Quark content of the nucleon in QCD: Perturbative and nonperturbative aspects

N. G. Stefanis
Institut für Theoretische Physik II, Ruhr-Universität Bochum, D-4630 Bochum, Federal Republic of Germany
(Received 1 February 1988; revised manuscript received 19 June 1989)

We elaborate on two proposed model distribution amplitudes for the nucleon, based on perturbative light-cone QCD supplemented by QCD sum rules. The novel nonperturbative features of these amplitudes are discussed in detail. Reasonable predictions for the Dirac form factor of the proton and the neutron are obtained, paying particular attention to the treatment of the effective coupling constant $\alpha_s(Q^2)$ and the scale parameter $\Lambda_{\rm QCD}$. In addition, the stability properties of the sum rules for the moments of these model distribution amplitudes are analyzed. The range of values of the parameters entering the sum rules is estimated. Relying on expectation values of longitudinal-momentum fractions instead of moments, a heuristic interpretation of the physical content of the model distribution amplitudes is attempted.

I. INTRODUCTION

One of the most challenging and fundamental questions of subnuclear physics is the understanding of the bound-state dynamics of the hadrons in terms of their quark and gluon degrees of freedom within quantum chromodynamics (QCD). In the last few years, the application of perturbative QCD to various[1-7] high-momentum-transfer exclusive processes involving hadrons has focused particular interest. The basic feature of such a process is the property of factorization[1,8-10] which allows the separation of short- and long-distance effects[11] via a Wilson[12] operator-product expansion[9] (OPE). Using the Brodsky-Lepage scheme[1] (see also Refs. 2 and 10), it is possible to express the hadronic amplitude as the convolution of a hard-scattering part $T_H(x_i,y_i,Q^2)$ calculable within perturbative QCD, and a wave-function part $\Phi(x_i,Q^2)$ which contains the (nonperturbative) binding effects of the hadron's constituents.

T_H corresponds to the coefficient function in the OPE and controls the scattering of the valence quarks from the initial to the final directions. The distribution amplitude[13] (modulo logarithmic corrections)

$$\Phi(x_i,Q^2)=\int^{k_{\perp i}^2\le Q^2}[d^2k_\perp]\psi(x_i,\mathbf{k}_{\perp i}) \tag{1.1}$$

with

$$[d^2k_\perp]\equiv 16\pi^3\delta^{(2)}\left[\sum_{i=1}^{n}k_{\perp i}\right]\prod_{i=1}^{n}\frac{d^2k_{\perp i}}{16\pi^3}$$

is the probability amplitude at some resolution scale Q^2 for finding the valence quarks carrying light-cone fractions of the hadron's momentum, $x_i=k_i^+/p^+=(k^0+k^3)_i/(p^0+p^3)$, integrated over transverse momenta $k_{\perp i}^2\le Q^2=-q^2$ where $p^\mu=(p^+,p^-,\mathbf{p}_\perp)$ is the momentum of the hadron. It is assumed that at large Q^2, i.e., asymptotically, the hard-scattering amplitude dominates over the soft contributions,[1] although the transition scale is still controversial.[5,14]

Recalling the OPE, $\Phi(x_i,Q^2)$ represents the nonvanishing hadronic matrix elements of the lowest-twist operators with respect to the (unknown) QCD physical vacuum. Until recently,[5,15,16] it was not possible to go beyond perturbative QCD and calculate realistic distribution amplitudes rigorously.[17] The situation improved considerably after the development of QCD sum rules initiated in 1979 by Shifman, Vainshtein, and Zakharov[18] (SVZ). Referring to their work, the nontrivial structure of the QCD physical vacuum manifests itself through field condensates, i.e., nonvanishing vacuum expectation values such as $\langle\Omega|\bar{q}q|\Omega\rangle$ and $\langle\Omega|G^i_{\mu\nu}G^i_{\mu\nu}|\Omega\rangle$, where $G^i_{\mu\nu}$ is the gluon field tensor, $\bar{q}$ and q denote (light) quark fields, and Ω stands for the physical vacuum of QCD. The condensates are of nonperturbative nature in the sense that they retain finite values *once* the divergent terms obtained in perturbation theory are removed by renormalization.[19] Their "standard" values, extracted from current algebra and instanton calculus, are[18]

$$\begin{aligned}&\left\langle\frac{\alpha_s}{\pi}G^2_{\mu\nu}\right\rangle\approx 1.2\times10^{-2}\ \text{GeV}^4\ ,\\ &\langle\sqrt{\alpha_s}\,\bar{u}u\rangle^2\approx\langle\sqrt{\alpha_s}\,\bar{d}d\rangle^2\approx 1.8\times10^{-4}\ \text{GeV}^6\ .\end{aligned} \tag{1.2}$$

The crucial step in the evaluation of model distribution amplitudes for hadrons was done by Chernyak, Zhitnitsky, and Zhitnitsky[5,20] (CZ). Using as a theoretical basis the eigenfunctions of the evolution equation,[1] they reconstructed a nucleon distribution amplitude from its lowest moments, which they estimated by means of QCD sum rules. The main results of their analysis are[5] (i) a pronounced flavor asymmetry of the nucleon distribution amplitude that is predicted to persist up to tremendously large momentum transfers and (ii) the correct sign and *seemingly* correct absolute values of the proton and neutron magnetic form factors. A recent reanalysis by King and Sachrajda[16] (KS) essentially confirms these findings, though the range of the moment sum rules is shifted.

Concerning the determination of the nucleon distribution amplitude via its moments, it is well known (from the classical theory of moments[21]) that a finite set of (actually lowest-order) moments cannot provide a unique

solution. Nevertheless, one might perhaps *naively* expect that the range of moment values allowed by QCD sum rules is strongly limited, rendering the variation of possible distribution amplitudes small. This however is not the case, as pointed out in Ref. 22. The reason can be traced to several uncertainties entering the calculation of higher moments.[5,23] While the lowest moments can be computed independently using, e.g., uncorrected vertex functions[24] or lattice gauge theory,[17] the calculation of the higher-order moments has still not been accomplished.[25] As a result, there is actually an infinite number of possible distribution amplitudes satisfying the CZ sum-rule constraints, but differing dramatically in their shapes and form-factor predictions.[22] This variation is inherent in the construction technique[5] of the nucleon distribution amplitude and has to be distinguished from other uncertainties due to the choice of $\Lambda_{\rm QCD}$ and the value of the "proton decay constant" f_N.

In Refs. 15 and 22 an alternative nucleon distribution amplitude was proposed by Gari and the present author (denoted GS in the following), selected to yield at some fixed reference momentum the lowest possible value of the ratio $|F_1^n/F_1^p|$. (F_1^p and F_1^n are the Dirac, i.e., helicity-conserving, form factors of the proton and the neutron, respectively.) While the CZ model uses for the representation of the nucleon distribution amplitude only the lowest-order Appell polynomials,[1,26] our model takes into account *all* Appell polynomials corresponding to a total of two derivatives in the interpolating operators used in the sum rules. Then the functional form of the nucleon distribution amplitude is strongly restricted and the form-factor predictions are in good agreement with the new high-Q^2 G_M^p data,[27] favoring the possibility that $F_1^n \approx 0$ in the whole Q^2 range.[28,29] In contrast, the CZ (KS) model predicts a large $|F_1^n|$ (compared to F_1^p), while the values predicted for F_1^p are comparable in size in all three models.[30]

More recently,[31] another promising possibility to select an optimal nucleon distribution amplitude was proposed, based on the relation $2\sqrt{2}\,G_M^{p\Delta^+} = 3G_M^p + 5G_M^n$, which is effectively a correlation between G_M^n and the N-Δ transition form factor $G_M^{p\Delta^+}$. It was found that the CZ nucleon distribution amplitude corresponds to a large $|G_M^n|$ (compared to G_M^p), and a small $G_M^{p\Delta^+}$, whereas the GS nucleon distribution amplitude gives a small $|G_M^n|$ and a $G_M^{p\Delta^+}$ of the same order as G_M^p. A better separation of the electric (G_E^n) from the magnetic (G_M^n) form factor of the neutron, appearing to be feasible if G_E^n is big at high Q^2 (Ref. 32), would help to verify the validity of these predictions.

Since the accuracy of the available form-factor data cannot exclude/favor one of the optional models [CZ (Ref. 5), GS (Ref. 15), KS (Ref. 16)], it would be desirable to have some other guide for selecting an optimal nucleon distribution amplitude. It is one of the major purposes of this paper to provide a more precise understanding of the reliability of a given distribution amplitude, by investigating the stability properties of the sum rules for its moments.

The remainder of the paper is organized as follows. In Sec. II we sketch the general formalism for calculating form factors in perturbative QCD[1,2] in connection with the sum-rule technique for the evaluation of the quark distribution amplitudes for the nucleon.[5] Section III is devoted to a systematic and detailed discussion of the nucleon distribution amplitude represented as a decomposition in terms of Appell polynomials. The specific features of the GS and the CZ quark distribution amplitudes are figured out and the corresponding proton and neutron Dirac form factors are calculated.

Section IV contains the stability analysis of the moment sum rules. We utilize the Wilson coefficients computed by CZ[5] to minimize the disparity in the sum rule for each moment using the nucleon residue (coupling) as input and regarding the nucleon mass and the duality interval (i.e., the continuum threshold) as tunable parameters to be determined from the optimal agreement of each sum rule. Two saturation models are considered. First, saturation of the phenomenological side of the sum rules by the lowest resonance (the nucleon) and second, saturation by taking into account a second "effective resonance" with mass $M_R = 1.5$ GeV. In the second case the residues of the "effective resonance" are also estimated. In performing this analysis we follow similar lines as Ioffe and Belyaev in their determination of baryon and baryon-resonance masses from QCD sum rules.[33]

In Sec. V we consider expectation values of longitudinal-momentum fractions and comment on the (heuristic) physical picture emerging from proposed nucleon distribution amplitudes raising objections against the popular probabilistic interpretation of moments (see, e.g., Refs. 5, 16, and 30). Finally Sec. VI gives a summary of our basic results and outlines the conclusions. This paper is partly an elaboration of results presented in Refs. 15 and 22.

II. THEORETICAL CONSIDERATIONS

A. Perturbative aspects

In perturbative light-cone QCD the magnetic form factor of the nucleon can be written in the factorized form[1]

$$G_M^N(Q^2) = \int_0^1 [dx] \int_0^1 [dy] \Phi^\dagger(y_i, \tilde{Q}_y) T_H(x_i, y_i, Q) \Phi(x_i, \tilde{Q}_x) \,, \tag{2.1}$$

where

$$[dx] = \delta \left[1 - \sum_{i=1}^{3} x_i \right] \prod_{i=1}^{3} dx_i$$

and

$$\tilde{Q}_x = \min_i (x_i Q) \,,$$

with analogous definitions for $[dy]$ and $\tilde{Q}_y$. T_H is a three-particle irreducible amplitude in the nucleon channels and represents the sum of all Born diagrams contributing to the process $\gamma^* + 3q \to 3q$, where the nucleon is replaced by three collinear (massless) valence quarks.

The function Φ ($\Phi^\dagger$) is the distribution amplitude for finding three valence quarks in the incoming (outgoing)

nucleon which are collinear up to a scale $\tilde{Q}_x^2$ ($\tilde{Q}_y^2$). The Q^2 variation of the nucleon distribution amplitude is weak and can be computed via the evolution equation.[1] The general solution of this equation is

$$\Phi(x_i,Q^2)=x_1x_2x_3\sum_{n=0}^{\infty}a_n\tilde{\Phi}_n(x_i)[\ln(Q^2/\Lambda_{\rm QCD}^2)]^{-\gamma_n}\ , \tag{2.2}$$

where γ_n are the anomalous dimensions of multiplicatively renormalizable three-quark operators with n derivatives interpolating between the nucleon and the vacuum, and the functions $\tilde{\Phi}_n(x_i)$ are the corresponding eigensolutions constituting a complete, orthogonal polynomial basis (Appell polynomials[34]). The one-loop values of γ_n and the Appell polynomials corresponding to a total of zero, one, and two derivatives in the interpolating operators are listed in Ref. 1 (see also Refs. 26, 35, and 36). The essential nonperturbative input in Eq. (2.2) are the coefficients a_n. Their determination will be treated in conjunction with the sum-rule technique in the next section.

Inserting solution (2.2) in Eq. (2.1), the nucleon magnetic form factor at large Q^2 takes the form

$$G_M^N(Q^2)\propto[\alpha_s^2(Q^2)/Q^4]\sum_{n,m=0}^{\infty}b_{nm}[\ln(Q^2/\Lambda_{\rm QCD}^2)]^{-\gamma_n-\gamma_m}[1+O(\alpha_s(Q^2),m^2/Q^2)]\ , \tag{2.3}$$

where the coefficients b_{nm} are determined from the value of the nucleon distribution amplitude $\Phi(x_i,Q_0^2)$ at the initial point of evolution, denoted by Q_0^2, and m^2/Q^2 stands for power-suppressed mass corrections. For asymptotically large Q^2, the form factor given in (2.3) is effectively dominated by the three-quark operator with the least number of derivatives. The corresponding lowest anomalous dimension for $SU(3)_c$ and three flavors is $\gamma_0=2/27$. Furthermore, $G_m^{p(n)}=F_1^{p(n)}(Q^2)+F_2^{p(n)}(Q^2)$ becomes asymptotically ($Q^2\to\infty$) identical with the helicity-conserving part $F_1^{p(n)}$, because the helicity-changing (Pauli) form factor $F_2^{p}(n)$ is power suppressed.[1] Thus the asymptotic form of $G_M^{p(n)}$, predicted by perturbative QCD, is

$$G_M^{p(n)}(Q^2)\to F_1^{p(n)}(Q^2)\propto[\alpha_s^2(Q^2)/Q^4][\ln(Q^2/\Lambda_{\rm QCD}^2)]^{-4/27}\ . \tag{2.4}$$

On the other hand, $\Phi(x_i,Q^2)$ becomes asymptotically totally symmetric under particle exchange, tending to the flavor-spin structure assumed in the SU(6)-symmetric quark model. According to Eq. (2.2), the asymptotic form of the nucleon distribution amplitude is[1]

$$\Phi_{\rm as}(x_i)=120x_1x_2x_3\ . \tag{2.5}$$

In order to extrapolate from the asymptotic to the intermediate/low Q^2 regime where the nonperturbative features of QCD become significant, detailed knowledge of the explicit structure of the amplitude $\Phi(x_i,Q^2)$ is needed.

B. Nonperturbative aspects

To proceed, consider the gauge-invariant (path-dependent) matrix element of three quark operators in Euclidean space:

$$\left\langle 0\left|\left[P\exp\left[-ig\int_{z_1(\Gamma_1)}^{z_3}A_\mu(\omega)d\omega_\mu\right]u_\alpha(z_1)\right]^a\left[P\exp\left[-ig\int_{z_2(\Gamma_2)}^{z_3}A_\nu(\omega')d\omega_\nu'\right]u_\beta(z_2)\right]^b d_\gamma^c(z_3)\right|p\right\rangle\epsilon^{abc}\ , \tag{2.6}$$

where a,b,c and α,β,γ are, respectively, color and spin labels, and $A_\mu(x)=\sum_{i=1}^8A_\mu^i(x)t^i$ are the Lie-algebra-valued gluon fields [t^i being the generators of SU(3)]. The path-ordering prescription P controls the expansion of the exponential integrals containing noncommuting variables: The integrations have to be performed along the path Γ_1 (Γ_2) leading from point z_1 (z_2) to point z_3 (Ref. 37).

We are interested in the evaluation of the above matrix element for a hard exclusive process where the virtual photon carries a large transverse momentum $q_\perp^2=-q^2\equiv Q^2\to\infty$. Since the exchange of large $q_\perp^2$ in the hard-scattering amplitude T_H occurs when the relative separation of the quark constituents approaches the light cone, we have $(z_i-z_j)^2\approx(z_{\perp i}-z_{\perp j})^2\to O(1/Q^2)$, where $z_{\mu i}\to z_in_\mu$ ($i=1,2,3$) and n_μ is the lightlike vector ($n^2=0$) (Ref. 1). Thus the leading- (lowest-)twist part can be projected out in (2.6) by the lightlike vector n_μ employing the light-cone gauge $n\cdot A=A^\dagger=0$. By virtue of this gauge,[38] the exponential factors in (2.6) reduce to unity, and the path-dependent matrix element simplifies to a trilocal, twist-three quantity[2,9] depending on three functions of positive parity V, A, and T (Ref. 39):

$$\langle 0|u_\alpha^a(z_1)u_\beta^b(z_2)d_\gamma^c(z_3)|p\rangle\epsilon^{abc}=\tfrac{1}{4}f_N[(\not{p}C)_{\alpha\beta}(\gamma_5N)_\gamma V(z_i\cdot p)+(\not{p}\gamma_5C)_{\alpha\beta}N_\gamma A(z_i\cdot p)-(\sigma_{\mu\nu}p_\nu C)_{\alpha\beta}(\gamma_\mu\gamma_5N)_\gamma T(z_i\cdot p)]\ ,$$

$$\not{p}=p_\mu\gamma_\mu,\quad \sigma_{\mu\nu}=\tfrac{1}{2}[\gamma_\mu,\gamma_\nu]\ . \tag{2.7}$$

Here $|p\rangle$ is the proton state with momentum p, N denotes the proton spinor, and C is the charge-conjugation matrix. The "proton decay constant" f_N (Refs. 5 and 33) is a dimensional quantity determining the value of the nucleon distribution amplitude at the origin.

In order to obtain the relation between the nucleon distribution amplitude Φ, defined in (1.1), and the trilocal matrix element (2.7), we have to Fourier transform the amplitudes V, A, and T according to

$$V(z_i\cdot p)=\int_0^1[dx]\exp\left[-i\sum_{i=1}^{3}x_i(z_i\cdot p)\right]V(x_i) \tag{2.8}$$

(analogously for A and T). The variables conjugate to the light-cone positions of the quark operators in (2.7) are collinear momentum fractions, i.e., the longitudinal momenta x_i with $0\le x_i\le 1$, $\sum_{i=1}^{3}x_i=1$ in the frame with $p_3\to\infty$. Accordingly, the scalar functions $V(x_i)$, $A(x_i)$, and $T(x_i)$ are distribution amplitudes controlling the longitudinal-momentum distributions of the valence quarks in the nucleon at fixed scale Q^2. They form, however, a redundant system, since they are interrelated by symmetries. Indeed, in the limit of strict collinear symmetry, combination of spin and flavor leads to the symmetry properties

$$\begin{aligned}&V(1,2,3)=V(2,1,3)\ ,\\ &A(1,2,3)=-A(2,1,3)\ ,\\ &T(1,2,3)=T(2,1,3)\ .\end{aligned} \tag{2.9}$$

On the other hand, the total isospin $\frac{1}{2}$ of the three-quark bound system requires

$$\begin{aligned}2T(1,2,3)=&V(1,3,2)-A(1,3,2)\\ &+V(2,3,1)-A(2,3,1)\ .\end{aligned} \tag{2.10}$$

Hence, the nucleon distribution amplitude may be expressed in terms of one mixed-symmetry amplitude, e.g.,[5]

$$\Phi_N(x_i)=V(x_i)-A(x_i)\ . \tag{2.11}$$

In the asymptotic limit ($Q^2\to\infty$), A becomes negligible (because of the Pauli principle) and V and T become totally symmetric under particle exchange so that $\Phi_N\to V\to\Phi_{\rm as}$, and $T\to\Phi_{\rm as}$, where $\Phi_{\rm as}$ is given by Eq. (2.5). The (weak) dependence of Φ_N at finite Q^2 manifests itself only via the factor

$$\left[\frac{\alpha_s(Q^2)}{\alpha_s(\mu^2)}\right]^{\gamma_n}=\left[\frac{\ln(Q^2/\Lambda^2_{\rm QCD})}{\ln(\mu^2/\Lambda^2_{\rm QCD})}\right]^{-\gamma_n}, \tag{2.12}$$

where γ_n are the anomalous dimensions mentioned previously, and the momentum scale μ^2 marks the normalization point. Since the three quarks in the process $\gamma^*+3q\to 3q$ have different virtualities $(1/k^2_{\perp i})\sim(1/x_iQ^2)$, there are different normalization scales to be matched and consequently the choice of μ^2 is ambiguous. However, on the basis of the extremely weak scale dependence of Φ_N, it is sufficient to use an average normalization point $\bar\mu^2$ whose value is determined by the characteristic virtuality of the constituents in the process (we return to this point in Sec. III). Thus the rate at which $\Phi_N(x_i,Q^2)$ approaches its asymptotic form depends strongly on its initial value $\Phi_N(x_i,\mu^2)$.

It is clear that the main point of concern is a realistic approximation for $\Phi_N(x_i,\mu^2)$. Since this has been discussed elsewhere,[5,16] we only sketch the conceptual essentials relevant to the present investigation. One considers correlation functions of the general form

$$i\int d^4x\, e^{iq\cdot x}\langle\Omega|T\{O_\gamma^{(n_1n_2n_3)}(x)[J_{\gamma'}^{(n_1)}(0)]^\dagger\}|\Omega\rangle \not{z}_{\gamma'\gamma}\ , \tag{2.13}$$

where $O_\gamma^{(n_1n_2n_3)}$ typifies operators such as

$$V_\gamma^{(n_1n_2n_3)}(0)=[(iz_\mu D_\mu)^{n_1}u(0)]^a C\not{z}[(iz_\nu D_\nu)^{n_2}u(0)]^b\{(iz_\sigma D_\sigma)^{n_3}[\gamma_5 d(0)]_\gamma\}^c\epsilon^{abc}\ , \tag{2.14}$$

$z^2=0$, $D_\mu=\partial_\mu-igA^i_\mu\lambda_i/2$, with similar definitions for $A_\gamma^{(n_1n_2n_3)}$ and $T_\gamma^{(n_1n_2n_3)}$. Their matrix elements $\langle\Omega|O_\gamma^{(n_1n_2n_3)}|p\rangle$ at fixed reference momentum μ^2 give the moments of the distribution amplitudes introduced in Eq. (2.7): for instance,[40]

$$\langle\Omega|V_\gamma^{(n_1n_2n_3)}(0)|p\rangle=f_N(z\cdot p)^{n_1+n_2+n_3+1}N_\gamma V^{(n_1n_2n_3)}\ , \tag{2.15}$$

and analogous expressions for $A^{(n_1n_2n_3)}$ and $T^{(n_1n_2n_3)}$.

The current $J_{\gamma'}^{(n_1)}(0)$ in (2.13) is an auxiliary local operator with isospin $\frac{1}{2}$ chosen to ensure dominance of the proton in the correlator.[41] Chernyak and Zhitnitsky[5] use the current

$$J_\gamma^{(n_1)}(0)=[(iz_\mu D_\mu)^{n_1}u(0)]^a C\not{z}u^b(0)\{[\gamma_5 d(0)]_\gamma\}^c\epsilon^{abc}\ , \tag{2.16}$$

whose matrix element $\langle\Omega|J_\gamma^{(n_1)}(0)|p\rangle$ is related to a mixture of moments:

$$\langle\Omega|J_\gamma^{(n_1)}(0)|p\rangle=f_N(z\cdot p)^{n_1+1}N_\gamma(\tfrac{1}{2}\Phi_N^{(n_100)}+T^{(n_100)})\ . \tag{2.17}$$

This correlator is essentially a two-point function composed of two local nucleon currents with extra derivatives.

To determine the moments of the nucleon distribution amplitude, the following correlators are evaluated in the spacelike region $q^2<0$ by employing the Fock-Schwinger gauge $x_\mu A_\mu=0$ (Ref. 42):

$$I^{(n_1n_2n_3)}(q,z)=i\int d^4x\, e^{iq\cdot x}\langle\Omega|T\{O_\gamma^{(n_1n_2n_3)}(x)[J_{\gamma'}^{(1)}(0)]^\dagger\}|\Omega\rangle \not{z}_{\gamma'\gamma}$$
$$=(z\cdot q)^{n_1+n_2+n_3+3}I^{(n_1n_2n_3)}(q^2) \tag{2.18}$$

and

$$K^{(n_1n_2n_3)}(q,z)=i\int d^4x\, e^{iq\cdot x}\langle\Omega|T\{T_\gamma^{(n_1n_2n_3)}(x)[J_{\gamma'}^{(0)}(0)]^\dagger\}|\Omega\rangle \not{z}_{\gamma'\gamma}$$
$$=(z\cdot q)^{n_1+n_2+n_3+3}K^{(n_1n_2n_3)}(q^2)\ . \tag{2.19}$$

Here $O_\gamma^{(n_1n_2n_3)}$ stands for one of the operators $\Phi_{N,\gamma}^{(n_1n_2n_3)}$, $V_\gamma^{(n_1n_2n_3)}$, and $A_\gamma^{(n_1n_2n_3)}$, specified above. The operator $T_\gamma^{(n_1n_2n_3)}$ refers to the distribution amplitude $T(x_i)$, which is related to the nucleon distribution amplitude $\Phi_N(x_i)$ by $2T(1,2,3)=\Phi_N(1,3,2)+\Phi_N(2,3,1)$.

The corresponding Borel-improved[18] moment sum rules (M^2 denotes the Borel parameter) are[5]

$$4|f_N|^2(\tfrac{1}{2}\Phi_N^{(100)}+T^{(100)})\Phi^{(n_1n_2n_3)}\exp(-M_N^2/M^2)=\frac{\beta_1^{(n_1n_2n_3)}}{160\pi^4}M^4[1-(1+H)e^{-H}]+\frac{\beta_2^{(n_1n_2n_3)}}{48\pi^2}\left\langle\Omega\left|\frac{\alpha_s}{\pi}G_{\mu\nu}^2\right|\Omega\right\rangle$$
$$+\frac{\beta_3^{(n_1n_2n_3)}}{3^5\pi M^2}\langle\Omega|\sqrt{\alpha_s}\,\bar{u}u|\Omega\rangle^2 \tag{2.20}$$

and

$$12|f_N|^2T^{(n_1n_2n_3)}\exp(-M_N^2/M^2)=\frac{\alpha_1^{(n_1n_2n_3)}}{80\pi^4}M^4[1-(1+H)e^{-H}]+\frac{\alpha_2^{(n_1n_2n_3)}}{48\pi^2}\left\langle\Omega\left|\frac{\alpha_s}{\pi}G_{\mu\nu}^2\right|\Omega\right\rangle$$
$$+\frac{\alpha_3^{(n_1n_2n_3)}}{3^5\pi M^2}\langle\Omega|\sqrt{\alpha_s}\,\bar{u}u|\Omega\rangle^2\ , \tag{2.21}$$

where $H=s^{(n_1n_2n_3)}/M^2$, $s^{(n_1n_2n_3)}$ being the appropriate duality interval for every moment, and M_N is the nucleon mass.

In Sec. IV we will treat Eq. (2.20) in more detail. Here, we only wish to make some clarifying remarks. The above sum rules include three types of contributions which are represented diagramatically in Fig. 1. The zeroth-order term of the operator expansion ($d=0$) is the perturbative contribution with Wilson coefficients $\beta_1^{(n_1n_2n_3)}$ and $\alpha_1^{(n_1n_2n_3)}$ [diagram (a) of Fig. 1]. The next nonvanishing contributions have dimensionality $d=4$ [diagrams of type (b) in Fig. 1] and represent nonperturbative corrections proportional to the gluon condensate $\langle\Omega|G_{\mu\nu}^2|\Omega\rangle$ (coefficients $\beta_2^{(n_1n_2n_3)}$ and $\alpha_2^{(n_1n_2n_3)}$). The diagrams of type (c) ($d=5$) and type (d) ($d=6$) give nonperturbative corrections proportional to the four-quark condensate $\langle\Omega|\bar{u}u|\Omega\rangle^2$, where the factorization hypothesis is used.[18] Their contributions are incorporated in the coefficients $\beta_3^{(n_1n_2n_3)}$ and $\alpha_3^{(n_1n_2n_3)}$. Note that the tree quark diagrams give zero contribution to the leading twist correlators considered above.[5] For example, the first term of the operator expansion with dimensionality $d=3$, proportional to the quark condensate $\langle\Omega|\bar{u}u|\Omega\rangle$, gives zero contribution to twist three. It is also worth noting that the coefficients $\beta_1^{(n_1n_2n_3)}$ and $\alpha_1^{(n_1n_2n_3)}$ calculated by CZ[5] coincide with those of KS.[16] On the contrary, there are severe discrepancies between the results published by these groups concerning the Wilson coefficients for the nonperturbative corrections.

III. RESULTS

A. Quark distribution amplitudes for the nucleon

We now proceed to evaluate the quark distribution amplitudes V, A, and T. In terms of these functions, the helicity-conserving color-singlet proton Fock state to leading twist (twist three) is written[1,2,5]

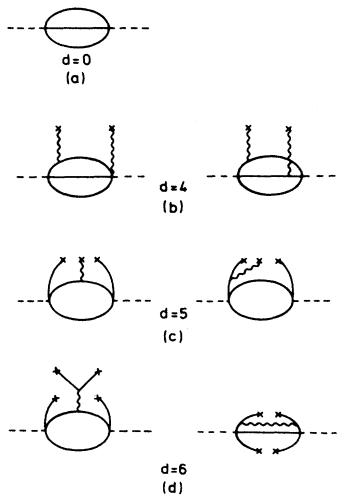

FIG. 1. Examples of diagrams contributing to the sum rules considered by CZ (Ref. 5). A cross ($\times$) attached to a quark (gluon) line indicates that the quark (gluon) goes into the corresponding condensate.

$$|p^{\uparrow}\rangle = \text{const} \times \int_0^1 [dx] \{ \tfrac{1}{2}[V(x_i) - A(x_i)] |u^{\uparrow}(x_1) u^{\downarrow}(x_2) d^{\uparrow}(x_3)\rangle + \tfrac{1}{2}[V(x_i) + A(x_i)] |u^{\downarrow}(x_1) u^{\uparrow}(x_2) d^{\uparrow}(x_3)\rangle - T(x_i) |u^{\uparrow}(x_1) u^{\uparrow}(x_2) d^{\downarrow}(x_3)\rangle \} \ . \tag{3.1}$$

The corresponding neutron Fock state is obtained from (3.1) by interchanging u and d, with an overall change of sign.

To determine the nucleon distribution amplitude we make the ansatz

$$\Phi_{\text{nucleon}}(x_i,\mu^2) = \Phi_{\text{as}}(x_i) \Phi_{\text{nonpert}}(x_i,\mu^2) \tag{3.2}$$

at a fixed-momentum scale μ^2 together with the boundary condition

$$\lim_{\mu^2 \to \infty} \Phi_{\text{nucleon}}(x_i,\mu^2) = \Phi_{\text{as}}(x_i) \ . \tag{3.3}$$

On the theoretical basis of the evolution equation,[1] we express the solution for $\Phi_{\text{nonpert}}(x_i,\mu^2)$ as an expansion in terms of Appell polynomials[43] (these constitute an orthogonal polynomial set on the triangle):

$$\Phi_{\text{nonpert}}(x_i)_{\mu^2} = \sum_{n=0}^{5} B_n|_{\mu^2} \widetilde{\Phi}_n(x_i) + \Delta\Phi \ . \tag{3.4}$$

The momentum μ^2 is taken to be the characteristic normalization scale (to be specified later), and the $\{\widetilde{\Phi}_n(x_i)\}$ are the first six Appell polynomials.[44] Having found the coefficients B_n at the point μ^2, their evolution to some arbitrary momentum Q^2 is controlled by the anomalous dimensions γ_n, according to

$$B_n(Q^2) = B_n(\mu^2) \left[\frac{\alpha_s(Q^2)}{\alpha_s(\mu^2)} \right]^{\gamma_n} \ . \tag{3.5}$$

The significant feature of our ansatz is that, truncating the (infinite) Appell polynomial series according to (3.4), the solution for Φ_{nonpert} incorporates properly *all* second-order (bilinear) polynomials $\widetilde{\Phi}_3$, $\widetilde{\Phi}_4$, and $\widetilde{\Phi}_5$. This treatment ensures that the functional representation of the nucleon distribution amplitude and the associated sum rules for its moments both correspond to matrix elements of interpolating operators with the same total of derivatives in the OPE.

We would like to stress, however, that the truncation of the Appell polynomial series to some fixed order n does not automatically imply or require an ordering of the expansion coefficients B_n. This is not a trivial point in view of statements[30] that a large coefficient B_5 may indicate the necessity to incorporate higher-order terms in the Appell polynomial decomposition reflecting in turn a reduced reliability of the nucleon distribution amplitude in question. In fact, we shall show below that the structure of $\Phi_{N/\text{GS}}$ is not specifically dominated by *one*, but rather by a cooperative combination of *all* second-order Appell polynomials, whereas the structure of $\Phi_{N/\text{CZ}}$ is practically insensitive to the inclusion of these contributions.

For a given scale μ^2, the moments of Φ_N are defined by

$$\Phi_N^{(n_1 n_2 n_3)} = \int_0^1 [dx] x_1^{n_1} x_2^{n_2} x_3^{n_3} \Phi_N(x_i) \tag{3.6}$$

with similar definitions for V, A, and T. Inserting expansion (3.4) into Eq. (3.6), one easily obtains the moments in terms of the six expansion coefficients B_n ($n = 0, \ldots, 5$). Actually it is more convenient to express the moments of Φ_N in terms of the moments of Φ_{as}:

$$\begin{aligned}
\Phi_N^{(n_1 n_2 n_3)} = {} & B_0 \Phi_{\text{as}}^{(n_1,n_2,n_3)} + B_1 (\Phi_{\text{as}}^{(n_1+1,n_2,n_3)} - \Phi_{\text{as}}^{(n_1,n_2,n_3+1)}) + B_2 (-3\Phi_{\text{as}}^{(n_1,n_2+1,n_3)} + \Phi_{\text{as}}^{(n_1,n_2,n_3)}) \\
& + B_3 (8\Phi_{\text{as}}^{(n_1+2,n_2,n_3)} + 8\Phi_{\text{as}}^{(n_1,n_2,n_3+2)} + 4\Phi_{\text{as}}^{(n_1+1,n_2,n_3+1)} + 7\Phi_{\text{as}}^{(n_1,n_2+1,n_3)} - 5\Phi_{\text{as}}^{(n_1,n_2,n_3)}) \\
& + B_4 (-\tfrac{4}{3}\Phi_{\text{as}}^{(n_1+2,n_2,n_3)} + \tfrac{4}{3}\Phi_{\text{as}}^{(n_1,n_2,n_3+2)} + \Phi_{\text{as}}^{(n_1+1,n_2,n_3)} - \Phi_{\text{as}}^{(n_1,n_2,n_3+1)}) \\
& + B_5 (\tfrac{14}{3}\Phi_{\text{as}}^{(n_1+2,n_2,n_3)} + \tfrac{14}{3}\Phi_{\text{as}}^{(n_1,n_2,n_3+2)} + 14\Phi_{\text{as}}^{(n_1+1,n_2,n_3+1)} + 7\Phi_{\text{as}}^{(n_1,n_2+1,n_3)} - 5\Phi_{\text{as}}^{(n_1,n_2,n_3)}) \ .
\end{aligned} \tag{3.7}$$

The results for the amplitudes Φ_N, V, and T together with the sum-rule constraints[5] are displayed in Tables I, II, and III, respectively.

The explicit expressions for the distribution amplitudes as functions of the coefficients B_n according to (3.4) are

$$\begin{aligned}
\Phi_N(x_i) = \Phi_{\text{as}}(x_i) [& (B_0 + B_2 - 5B_3 - 5B_5) + (B_1 + B_4)x_1 + (-3B_2 + 7B_3 + 7B_5)x_2 \\
& - (B_1 + B_4)x_3 + (4B_3 + 14B_5)x_1 x_3 + (8B_3 - \tfrac{4}{3}B_4 + \tfrac{14}{3}B_5)x_1^2 + (8B_3 + \tfrac{4}{3}B_4 + \tfrac{14}{3}B_5)x_3^2] \ ,
\end{aligned} \tag{3.8}$$

$$\begin{aligned}
V(x_i) = \Phi_{\text{as}}(x_i) [& (B_0 + B_2 - 5B_3 - 5B_5) + \tfrac{1}{2}(B_1 - 3B_2 + 11B_3 + B_4 + 21B_5)(x_1 + x_2) \\
& - (B_1 + B_4)x_3 - (4B_3 + 14B_5)x_1 x_2 + \tfrac{1}{6}(12B_3 - 4B_4 - 28B_5)(x_1^2 + x_2^2) \\
& + \tfrac{1}{3}(24B_3 + 4B_4 + 14B_5)x_3^2] \ ,
\end{aligned} \tag{3.9}$$

TABLE I. Moments of the nucleon distribution amplitude $\Phi_N(x_i)$ in terms of the expansion coefficients B_n. The sum-rule constraints of CZ are also shown.

$n_1n_2n_3$	$\Phi_N^{(n_1n_2n_3)}$	$\Phi_{N/(\mathrm{SR})}^{(n_1n_2n_3)}$
000	B_0	1
100	$\frac{1}{21}(7B_0+B_1+B_2)$	0.60–0.75
010	$\frac{1}{21}(7B_0-2B_2)$	0.09–0.16
001	$\frac{1}{21}(7B_0-B_1+B_2)$	0.18–0.24
200	$\frac{1}{756}(108B_0+27B_1+27B_2+9B_3-B_4-B_5)$	0.25–0.40
020	$\frac{1}{126}(18B_0-9B_2+B_3+B_5)$	0.03–0.08
002	$\frac{1}{756}(108B_0-27B_1+27B_2+9B_3+B_4-B_5)$	0.08–0.12
110	$\frac{1}{756}(72B_0+9B_1-9B_2-3B_3+B_4-3B_5)$	0.07–0.12
101	$\frac{1}{756}(72B_0+18B_2-6B_3+4B_5)$	0.09–0.14
011	$\frac{1}{756}(72B_0-9B_1-9B_2-3B_3-B_4-3B_5)$	−0.03–0.03

$$A(x_i)=\Phi_{\mathrm{as}}(x_i)[\tfrac{1}{2}(-B_1-3B_2+3B_3-B_4-7B_5)(x_1-x_2)+\tfrac{1}{6}(-12B_3+4B_4+28B_5)(x_1^2-x_2^2)]\ , \tag{3.10}$$

$$T(x_i)=\Phi_{\mathrm{as}}(x_i)[(B_0+B_2-5B_3-5B_5)+(-3B_2+7B_3+7B_5)x_3+(4B_3+14B_5)x_1x_2+(8B_3+\tfrac{14}{3}B_5)(x_1^2+x_2^2)]\ , \tag{3.11}$$

where the symmetry properties (2.9) and (2.10), and the relation $\sum_{i=1}^{3}x_i=1$ have been used to derive the amplitudes V, A, and T from Φ_N.

With the above distribution amplitudes, and Eq. (2.1), the nucleon Dirac form factor can be cast in the form[5]

$$Q^4F_1^N(Q^2)\approx\tfrac{1}{54}[4\pi\bar{\alpha}_s(Q^2)]^2|f_N|^2\int_0^1[dx]\int_0^1[dy]\left[2\sum_{i=1}^{7}e_iT_i(x,y)+\sum_{i=8}^{14}e_iT_i(x,y)\right]\ , \tag{3.12}$$

where e_i is the electric charge of the struck quark, and the x,y dependence of the effective coupling constant is neglected in favor of an average value $\bar{\alpha}_s$ taken outside the integrals. The amplitudes $T_i(x,y)=\Phi_i(x)T_H(x,y)\Phi_i(y)$ represent convolutions of T_H with the appropriate distribution amplitudes for each contributing diagram (indicated by the index i).

Integrating over x_i and y_i, the proton and neutron Dirac form factors in terms of the coefficients B_n are

$$Q^4F_1^p(Q^2)\approx\tfrac{1}{54}[4\pi\bar{\alpha}_s(Q^2)]^2|f_N|^2I^p \tag{3.13}$$

with

$$\begin{aligned}I^p=\tfrac{25}{243}(&0B_0^2+2160B_1^2+11\,664B_2^2+609\,12B_3^2+104B_4^2+2772B_5^2+13\,608B_0B_1+17\,496B_0B_2\\&+64\,152B_0B_3-3240B_0B_4-13\,608B_0B_5+9072B_1B_2+23\,760B_1B_3+936B_1B_4-3780B_1B_5\\&+46\,656B_2B_3-2376B_2B_4-3564B_2B_5-4968B_3B_4-19\,116B_3B_5+492B_4B_5)\end{aligned} \tag{3.14}$$

TABLE II. Moments of the nucleon distribution amplitude $V(x_i)$ in terms of the expansion coefficients B_n. The sum-rule constraints of CZ are also shown.

$n_1n_2n_3$	$V^{(n_1n_2n_3)}$	$V_{(\mathrm{SR})}^{(n_1n_2n_3)}$
000	B_0	1
100	$\frac{1}{42}(14B_0+B_1-B_2)$	0.38–0.42
010	$\frac{1}{42}(14B_0+B_1-B_2)$	0.38–0.42
001	$\frac{1}{21}(7B_0-B_1+B_2)$	0.18–0.24
200	$\frac{1}{1512}(216B_0+27B_1-27B_2+15B_3-B_4+5B_5)$	0.18–0.25
020	$\frac{1}{1512}(216B_0+27B_1-27B_2+15B_3-B_4+5B_5)$	0.18–0.25
002	$\frac{1}{756}(108B_0-27B_1+27B_2+9B_3+B_4-B_5)$	0.08–0.12
110	$\frac{1}{756}(72B_0+9B_1-9B_2-3B_3+B_4-3B_5)$	0.07–0.12
101	$\frac{1}{1512}(144B_0-9B_1+9B_2-9B_3-B_4+B_5)$	0.04–0.08
011	$\frac{1}{1512}(144B_0-9B_1+9B_2-9B_3-B_4+B_5)$	0.04–0.08

TABLE III. Moments of the nucleon distribution amplitude $T(x_i)$ in terms of the expansion coefficients B_n. The sum-rule constraints of CZ are also shown.

$n_1n_2n_3$	$T^{(n_1n_2n_3)}$	$T^{(n_1n_2n_3)}_{(SR)}$
000	B_0	1
100	$\frac{1}{21}(7B_0+B_2)$	0.40–0.50
010	$\frac{1}{21}(7B_0+B_2)$	0.40–0.50
001	$\frac{1}{21}(7B_0-2B_2)$	0.05–0.16
200	$\frac{1}{756}(108B_0+27B_2+9B_3-B_5)$	0.22–0.28
020	$\frac{1}{756}(108B_0+27B_2+9B_3-B_5)$	0.22–0.28
002	$\frac{1}{126}(18B_0-9B_2+B_3+B_5)$	0.02–0.06
110	$\frac{1}{756}(72B_0+18B_2-6B_3+4B_5)$	0.09–0.13
101	$\frac{1}{756}(72B_0-9B_2-3B_3-3B_5)$	0.04–0.08
011	$\frac{1}{756}(72B_0-9B_2-3B_3-3B_5)$	0.04–0.08

and

$$Q^4F_1^n(Q^2)\approx\tfrac{1}{54}[4\pi\bar{\alpha}_s(Q^2)]^2|f_N|^2I^n \tag{3.15}$$

with

$$\begin{aligned}I^n=\tfrac{25}{243}(&17\,496B_0^2+2376B_1^2-1944B_2^2-18\,360B_3^2+104B_4^2-870B_5^2-13\,608B_0B_1-17\,496B_0B_2\\&-9720B_0B_3+3240B_0B_4-6480B_0B_5-9072B_1B_2-23\,760B_1B_3-936B_1B_4+3780B_1B_5\\&-19\,440B_2B_3+2376B_2B_4+540B_2B_5+4968B_3B_4+7020B_3B_5-492B_4B_5)\ .\end{aligned} \tag{3.16}$$

Strictly speaking, expressions (3.12), (3.13), and (3.15) are not quite right because the Q^2 evolution of the form factors is governed not only by the momentum dependence of α_s, but also by the Q^2 variation of the coefficients B_n. However, their influence on the evolution is a minor effect [see Eq. (3.5)] and can be ignored in a first approximation. [Note that Q^2 logarithmic corrections due to anomalous dimensions have also not been introduced explicitly in the sum rules (2.20) and (2.21) (Ref. 5).]

Except for the coefficient B_0 which is fixed upon the normalization condition

$$\int_0^1[dx]\Phi_N(x_i,\mu^2)=1\ , \tag{3.17}$$

the other coefficients can be determined by inverting the equations for the moments $\Phi_N^{(n_1n_2n_3)}$ using as input the sum-rule constraints (Table I). One observes that the simultaneous consistency of the sum rules for the linear moments requires $B_1^{\max}=5.05$, $B_1^{\min}=3.79$, $B_2^{\max}=2.55$, and $B_2^{\min}=1.83$. While the sum-rule constraints suffice to keep the variation of the allowed values for B_1 and B_2 small, a complete analysis[22] shows that they are not stringent enough to limit the variation in sign and magnitude of the higher-order coefficients B_3, B_4, and B_5. This variation is exemplified in Table IV by two admissible[22] nucleon distribution amplitudes (examples 1 and 2) in comparison with the model distribution amplitudes of CZ and GS (Ref. 45). Extending this discussion to the Dirac form factors F_1^p and F_1^n, the situation is quite analogous because of the sensitivity of I^p [Eq. (3.14)] and I^n [Eq. (3.16)] to the signs and magnitudes of the coefficients B_n. (Cancellations of this type were found also for the transition form factor $G_M^{p\Delta^+}$—see Refs. 7 and 31.)

Turn now to the model distribution amplitudes of CZ (Ref. 5) and GS (Refs. 15 and 22). Their physical content may become more transparent by illustration (Fig. 2). It is worth noting that there are substantial discrepancies between our graphical representation of the CZ amplitudes and that given in Ref. 5. Even allowing for different scales, the sharp peaks found there cannot be reproduced. In particular, our graphical representation effects the existence of negative domains in the CZ distribution amplitudes, domains which have been disregarded in the figures of Ref. 5. We emphasize this last point as a warning in case of attempting to extract any but the most qualitative conclusions from the graphics of Ref. 5 (cf. Sec. V).

In order to make the foregoing statements more precise, the top-elevation pattern of the quark distribution amplitudes on the Mandelstam plane spanned by x_1, x_2, and x_3 with the constraint $x_1+x_2+x_3=1$ is also exposed (Fig. 3). One notices that the maximum of V_{GS} coincides exactly with that of Φ_{as} at $x_i=\frac{1}{3}$. Since asymp-

TABLE IV. Coefficients B_n of the Appell polynomial expansion for four different nucleon distribution amplitudes specified in the text.

B_n	Example 1	Example 2	CZ	GS
B_0	1.0	1.0	1.0	1.0
B_1	3.9	4.0	4.305	4.105
B_2	1.9	2.0	1.925	2.06
B_3	1.3	1.95	2.247	−4.72
B_4	9.0	−5.0	−3.465	5.0
B_5	1.8	2.0	0.013	9.3

totically $\Phi_N \to V \to \Phi_{as}$, the GS model favors the possibility that the nonperturbative effects become significant predominantly near the edges of phase space, whereas the central region ($x_i \approx \frac{1}{3}$) is positive and practically unaffected by such effects. This should be contrasted to the reversed possibility offered by the CZ model (Figs. 2 and 3).

The differences between the two sets of model distribution amplitudes become more pronounced if one compares instead of the full amplitudes their nonperturbative parts (Fig. 4). Then one observes that the nonperturbative parts of the GS amplitudes have mainly *convex* contours, while the CZ counterparts are rather *concave* with "spikes" at the corners of phase space.

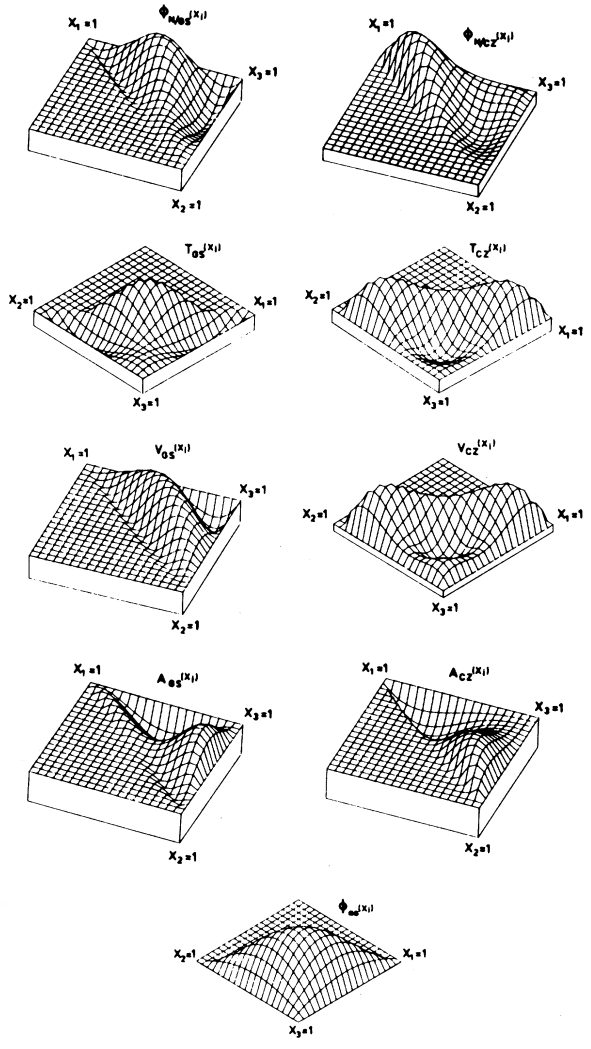

FIG. 2. Quark distribution amplitudes for the nucleon as three-dimensional surfaces over the plane spanned by x_1, x_2, and $x_3 = 1 - x_1 - x_2$ for two different models: GS amplitudes (left column); CZ amplitudes (right column). For comparison, the asymptotic solution is also shown. Note that for each figure the optimal perspective is chosen.

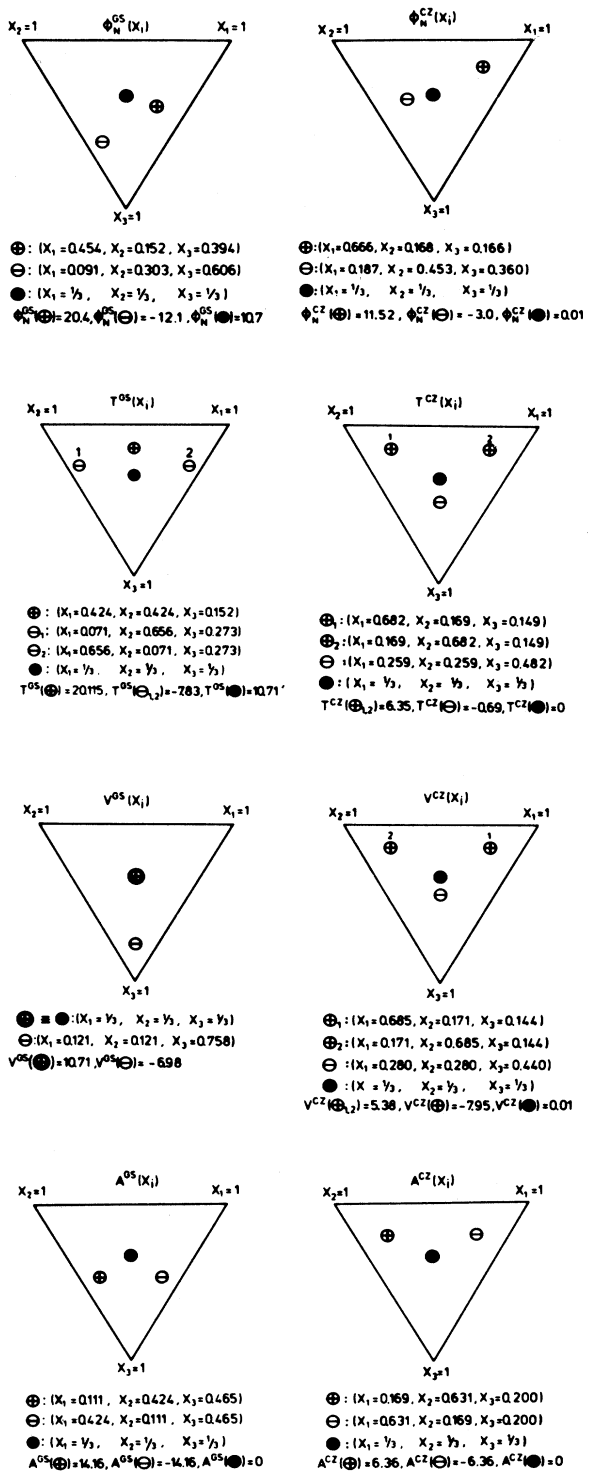

FIG. 3. Top-elevation pattern of the quark distribution amplitudes on the Mandelstam plane (equilateral triangle) for the variables x_1, x_2, and $x_3 = 1 - x_1 - x_2$. The left column shows the GS model, the right one the CZ model. Only the main maxima ($\oplus$) and main minima ($\ominus$) are indicated. In each plot the black dot marks the central point ($x_1 = x_2 = x_3 = \frac{1}{3}$) of the triangle where Φ_{as} has its maximal value.

The essence of the above discussion is that realistic distribution amplitudes which incorporate nonperturbative contributions have complex profiles that are accentuated by *nodes* and thus differ greatly from the "triune" structure of the asymptotic solution obtained in perturbative QCD.

At a more speculative level, one may argue that there is a tendency for the original coherence of Φ_{as} at asymptotic Q^2 to be lost and for the distribution amplitude Φ_N to become distorted in shape at finite Q^2 where the antisymmetric part A is not negligible. In a sense, the nonperturbative vacuum of QCD, populated by quark-gluon condensates, acts as a dispersive medium where different components of a wave propagate with different speeds and tend to change phase with respect to one another.

Having constructed model distribution amplitudes for the nucleon, it is now important to clarify the question about the respective contributions of the second-order Appell polynomials, according to ansatz (3.4). It is an instructive exercise to study the influence of the coefficients B_n $(n=3,4,5)$ on the shape of the amplitudes Φ_N by considering a *trial* nucleon distribution amplitude, truncated at $n=2$, i.e., setting in Eq. (3.8) $B_3=B_4=B_5=0$, and then include the second-order Appell polynomials corresponding to these coefficients successively.

We perform this analysis graphically (Fig. 5) considering the coefficients B_n $(n=3,4,5)$ to have fixed values: namely, either those calculated by CZ or those calculated by GS. Then it is obvious that the profile of the GS amplitude begins to deviate from that of the CZ amplitude only when bilinear Appell polynomials are included. By contrast, the inclusion of these terms does not exert a significant influence on the shape of the CZ amplitude. Since the polynomials $\tilde{\Phi}_3$, $\tilde{\Phi}_4$, and $\tilde{\Phi}_5$ are the first to contain terms $\propto x_i^2$ and $\propto x_i x_j$, their relative dominance in Φ_N^{GS} indicates strong correlations between the valence

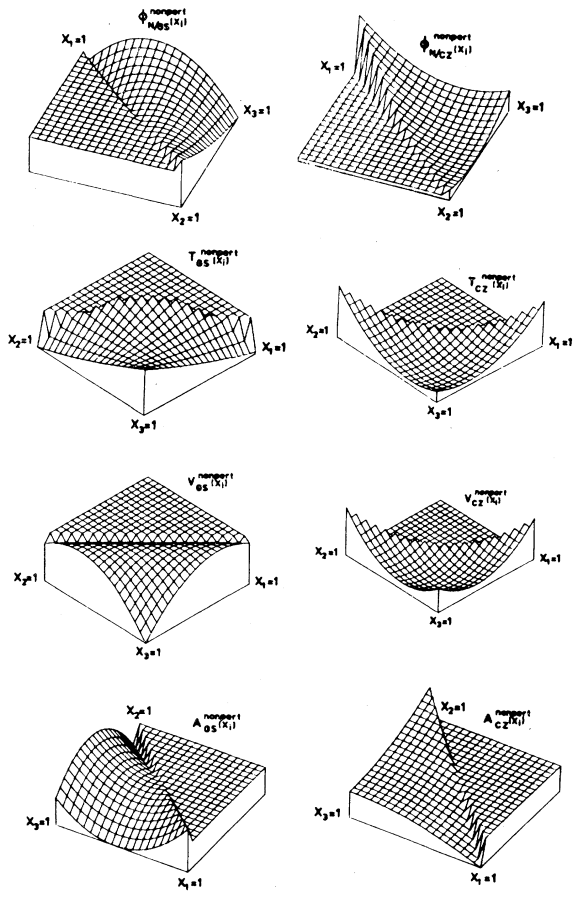

FIG. 4. Illustration of the nonperturbative parts of the nucleon distribution amplitude for two different models: GS model (left column); CZ model (right column). The physical region of phase space is the equilateral triangle with $x_1+x_2+x_3=1$.

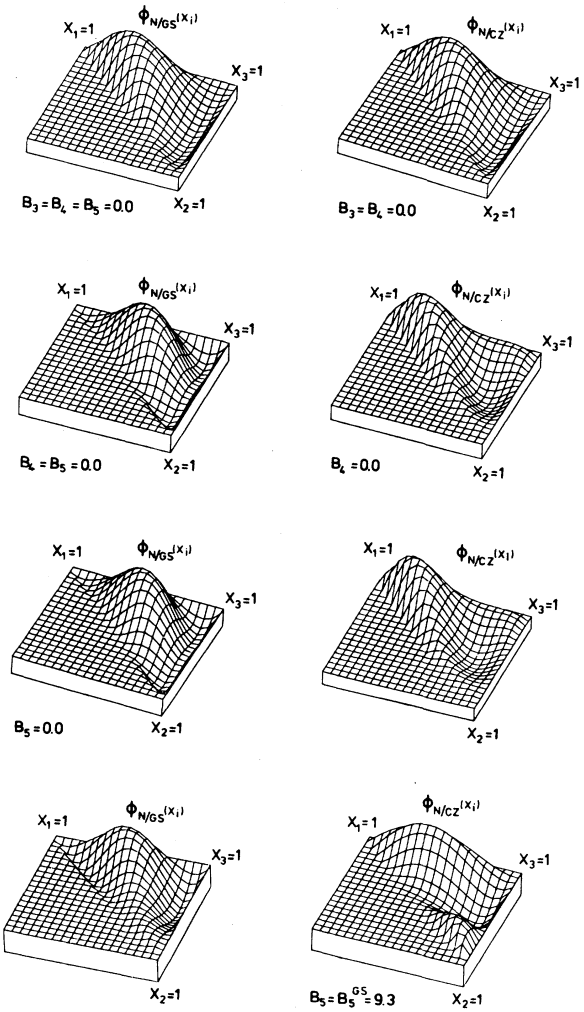

FIG. 5. Successive incorporation of the second-order Appell polynomials in the nucleon distribution amplitude Φ_N according to ansatz (3.4). The GS amplitude is shown in the left column. The right column contains the results for the CZ amplitude. The graph in the bottom right corner shows a spurious form of the CZ amplitude obtained by setting $B_5=B_5^{GS}=9.3$. Note that when the values of the coefficients B_n deviate from those given in Table IV, they are supplied in the figure.

quarks within the nucleon. Furthermore, it follows from Fig. 5 that the contours of Φ_N^{GS} are not particularly sensitive to the *separate* incorporation of $\tilde{\Phi}_5$, even with an expansion coefficient B_5 as large as $B_5^{GS}=9.3$ (see Table IV). The same is (almost) true also for the amplitude Φ_N^{CZ}. The graph in the bottom right corner of Fig. 5 shows a *spurious* amplitude Φ_N^{CZ}, in which the coefficient B_5 is taken to be nonzero and equal to $B_5^{GS}=9.3$. Although the profile of the original amplitude is distorted, its main characteristics are conserved.

The point of this exercise is that, relying in ansatz (3.4) exclusively on the zeroth- and first-order Appell polynomials $\tilde{\Phi}_0$, $\tilde{\Phi}_1$, and $\tilde{\Phi}_2$, the sum-rule constraints[5] actually *force* the nucleon distribution amplitude to have the functional form of Φ_N^{CZ}. Conversely, the inclusion of the second-order Appell polynomials $\tilde{\Phi}_3$, $\tilde{\Phi}_4$, and $\tilde{\Phi}_5$ in (3.4) favors a nucleon distribution amplitude with the structure of Φ_N^{GS}.

B. Dirac form factors of the nucleon

The results obtained in the preceding subsection are now applied to the evaluation of the nucleon form factor. The calculation of the helicity-conserving (Dirac) form factors F_1^p and F_1^n, according to Eqs. (3.13)–(3.16), yields two expressions which are represented graphically in Fig. 6 (proton) and Fig. 7 (neutron). These results have been obtained analytically under the assumption that the x,y dependence of the effective coupling constant can be ignored. The individual contributions to I^p [Eq. (3.14)] and I^n [Eq. (3.16)] of the diagrams of Ref. 5 are given in Table V.

In the case of the GS model, the dominant contributions come from diagrams 9 and 10 with gluon virtualities $Q^2(1-x_1)(1-y_1)$ and $Q^2x_2y_2$. Substituting the longitudinal momenta at the position of the main maximum of the amplitude T_{GS} (see Fig. 3), the averaged coupling strength is

$$\bar{\alpha}_s(Q^2)=[\alpha_s(Q^2\times 0.332)\alpha_s(Q^2\times 0.18)]^{1/2} . \quad (3.18)$$

In the case of the CZ model, diagram 1 dominates with gluon virtualities $Q^2(1-x_1)(1-y_1)$ and $Q^2x_3y_3$. Then it follows

$$\bar{\alpha}_s(Q^2)=[\alpha_s(Q^2\tfrac{1}{9})\alpha_s(Q^2\tfrac{1}{36})]^{1/2} , \quad (3.19)$$

where the coordinates in phase space of the main maximum of the amplitudes Φ_N^{CZ} are used (see Fig. 3).

In both cases the nominal value of Q^2 is large, but the *actual* value in the argument of $\bar{\alpha}_s$ is rescaled down to the intermediate or even low-Q^2 region because the appropriate gluon virtualities have to be used. The model predictions for F_1^p and F_1^n are labeled (1) and are presented, respectively, in Figs. 6 and 7. An improved treatment uses instead of a single average value $\bar{\alpha}_s$, for every contributing diagram to I^p (I^n) the respective coupling strength with the appropriate virtualities to obtain the curves marked (2) in Figs. 6 and 7 ($\Lambda_{QCD}=180$ MeV). Note that for the neutron only the theoretical predictions are shown because there is no experimental data in the high-Q^2 region.

It is clear that the form-factor predictions depend in a crucial way on the choice of the scale parameter Λ_{QCD}. A small value $\Lambda_{QCD}\approx 100$ MeV is sometimes preferred[1,5,30] because the smaller the scale parameter Λ_{QCD} the larger the distances for which the small-coupling expansion is valid. The value we have chosen, however, is more appropriate for form-factor calculations. In a recent publication[46] we showed that the $\ln Q^2$ dependence predicted by perturbative QCD can be *directly* tested looking at the plot versus Q^2 of the magnetic form factor G_M^p, which for $Q^2\to\infty$, i.e., asymptotically, becomes indistinguishable from the Dirac form factor F_1^p. The best fit to the G_M^p data[47] yielded for three flavors $\Lambda_{QCD}=180$ MeV corresponding to $(\chi^2/\text{data})=0.263$. (This semiphenomenological fit is also displayed in Fig. 6.)

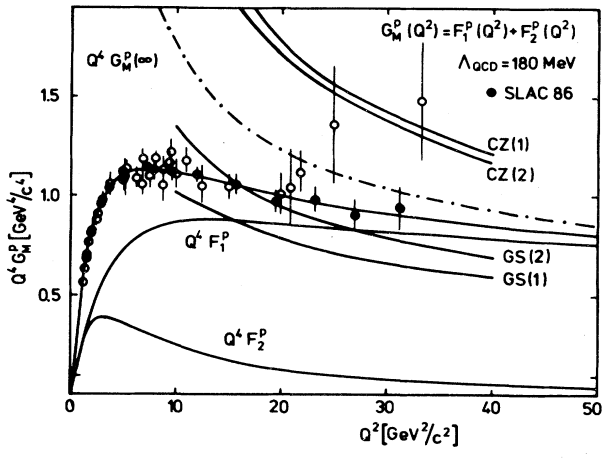

FIG. 6. Predictions for the proton Dirac form factor extracted from the GS and CZ models in comparison with the semiphenomenological fit of Ref. 46 and the existing G_M^p data (Ref. 47). The asymptotic prediction $[G_M^p(\infty)]$ of perturbative QCD (Ref. 1) is also shown. The curves labeled (1) and (2) are specified in the text.

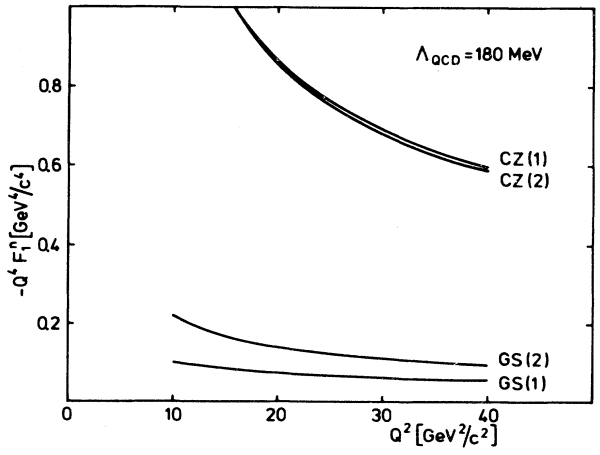

FIG. 7. Predictions for the neutron Dirac form factor extracted from the GS and CZ models by applying two different treatments for $\alpha_s(Q^2)$, as explained in the text.

TABLE V. Individual contributions to the proton and the neutron Dirac form factors calculated with the model distribution amplitudes of GS and CZ. An average value $\bar{\alpha}_s$ outside the integrals in Eq. (3.12) is assumed. The index i enumerates the diagrams given in Table I of Ref. 5.

i	$I^p_{i/\mathrm{GS}}$	$I^n_{i/\mathrm{GS}}$	$I^p_{i/\mathrm{CZ}}$	$I^n_{i/\mathrm{CZ}}$
1	19 108.52	−9554.26	139 309.65	−65.654.83
2	0	0	0	0
3	18 849.60	−9424.80	−93 753.33	46 876.67
4	413.41	−206.70	1209.03	−604.52
5	3980.72	−1990.36	−45 253.08	22 626.54
6	0	0	0	0
7	−32 031.30	64 062.60	−3282.07	6564.14
8	0	0	0	0
9	58 279.99	−29.140.0	62 243.27	−31 121.64
10	58 279.99	−29.140.0	62 243.27	−31 121.64
11	0	0	0	0
12	−491.01	982.03	1851.97	−3703.94
13	−663.05	1326.11	−1474.08	2984.17
14	−491.01	982.03	1851.97	−3703.94

Using instead of $\Lambda_{\mathrm{QCD}}=100$ MeV this scale in the one-loop expression for the coupling strength[48]

$$\alpha_s(Q^2)=\frac{4\pi}{\beta_0 \ln(Q^2/\Lambda^2_{\mathrm{QCD}})} \quad (Q^2 \gg \Lambda^2_{\mathrm{QCD}}) , \tag{3.20}$$

with $\beta_0=9$ (for three flavors), the model predictions of CZ for F^p_1 are shifted far away from the data (Fig. 6). In this context we remark that the theoretical predictions for F^p_1 in Fig. 6 should not be compared with the full G^p_M data, but rather with the curve for $Q^4F^p_1$. The reason is that the helicity-changing part of the magnetic form factor, i.e., the Pauli form factor F^p_2, is not necessarily equal to zero at moderate momenta, say, below 10 GeV^2 (Refs. 28 and 46).

Some other form factors calculated with the two models at fixed momentum[49] $Q^2=20$ GeV^2 and using the same value of the effective coupling constant, $\bar{\alpha}_s=0.3$, are supplied in Table VI. Allowing, however, for rescaled arguments in $\bar{\alpha}_s$, in accordance with the gluon virtualities appropriate for each model, the *deceptive* coincidence between $F^p_{1/\mathrm{GS}}$ and $F^p_{1/\mathrm{CZ}}$ in Table VI is removed, and one finds $Q^4F^p_{1/\mathrm{GS}}=0.78$ GeV^4, $Q^4F^p_{1/\mathrm{CZ}}=1.58$ GeV^4 for $\Lambda_{\mathrm{QCD}}=180$ MeV or $Q^4F^p_{1/\mathrm{GS}}=0.61$ GeV^4, $Q^4F^p_{1/\mathrm{CZ}}=0.89$ GeV^4 for $\Lambda_{\mathrm{QCD}}=100$ MeV.

Another important point is that the fitted curve $Q^4F^p_1$ in Fig. 6 scales much better than all theoretical predictions. This is because the Q^2 evolution of the calculated form factors is mainly due to the effective coupling constant given by (3.20). In order to improve the scaling behavior of the form factors, one has to treat $\alpha_s(Q^2)$ in a more accurate way. Such an attempt at treating α_s *inside* the integrals in (3.12) was recently reported by Ji, Sill, and Lombard-Nelsen[30] (JSLN). Owing to the fact that Eq. (3.20) becomes infinite at the end points of integration, they try to take account of the end-point contributions having recourse to a modified expression for α_s, proposed by Cornwall:[50]

$$\alpha_s(Q^2)=\frac{4\pi}{\beta_0 \ln[(Q^2+4m_g^2)/\Lambda^2_{\mathrm{QCD}}]} . \tag{3.21}$$

Here m_g is a dynamical or effective gluon mass with numerical values in the range 500±200 MeV (Ref. 50).

Technically, m_g is an infrared (IR) cutoff serving (implicitly) to regularize one of the gluon propagators becoming soft (compared to the photon momentum) along the boudaries of phase space, where some x_i is very small. It is clear that such a nonzero gluon mass will "freeze" the value of the effective coupling constant for $Q^2 \leq 4m_g^2$. The regulator role of m_g is more obvious when Eq. (3.21) is rewritten in the form[51]

$$\alpha_s(Q^2)=\frac{4\pi}{\beta_0 \ln[(Q^2+\lambda\Lambda^2_{\mathrm{QCD}})/\Lambda^2_{\mathrm{QCD}}]} , \tag{3.22}$$

where now λ is a purely phenomenological parameter ruling the "freezing" of the effective coupling constant at low Q^2. In fact, for values $Q^2 \leq \lambda\Lambda^2_{\mathrm{QCD}}$ the coupling constant ceases to increase and flattens out. Since a dynamically generated mass is not a constant but vanishes at large momentum (see Ref. 50 and references cited therein), the IR-regularized expressions (3.21) and (3.22) transform for large Q^2 into the conventional one.

Physically, the IR regularization of $\alpha_s(Q^2)$ means a sharp separation of short- from long-distance dynamics, which in turn implements that the long-range forces become saturated at some scale m_g^{-1}. Note, however, that

TABLE VI. Form-factor predictions extracted from four different nucleon distribution amplitudes specified in the text. The numbers in parentheses are the values given by CZ (Ref. 5). All values refer to $Q^2=20$ GeV^2, $\bar{\alpha}_s=0.3$, and $|f_N|=5.2\times10^{-3}$ GeV^2.

Form factors	Distribution amplitudes			
(GeV^4)	Example 1	Example 2	CZ	GS
$Q^4F^p_1$	0.29	0.68	0.89(1.17)	0.89
$Q^4F^n_1$	−0.124	−0.335	−0.43(−0.57)	−0.086
Q^4g_A	0.45	1.06	1.36	1.00
$Q^4G_{Mp\Delta^+}$	0.04	−0.03	0.01	0.72

a consistent treatment of the end-point region of phase space, where perturbation theory breaks down and nonleading contributions are important, should saturate the momentum transfer carried by the gluons not only *implicitly* in $\alpha_s(Q^2)$ but also *explicitly* in the gluon propagators, using the same IR cutoff. This has not been done in the JSLN analysis. Rather they treat m_g as an *independent* fit parameter that is adjusted to provide optimal agreement between the data and selected models for nucleon distribution amplitudes.

Using $\Lambda_{\rm QCD}=100$ MeV, they find $m_g^2=0.3$ GeV^2 [CZ, GS (Ref. 52) models], and $m_g^2=0.6$ GeV^2 (KS model). Although these results are consistent with the estimates of Cornwall,[50] and those of Cornwall and Soni[53] and the scaling behavior of the form factors is considerably improved, several comments are in order. First, according to Cornwall,[50] m_g and $\Lambda_{\rm QCD}$ are intimately *interrelated* by the consistency relation $m_g/\Lambda_{\rm QCD}\approx 1.5-2.0$ (or $\sqrt{\lambda}\approx 3-4$). The JSLN analysis clearly violates this condition, yielding $m_g^{\rm CZ(GS)}/\Lambda_{\rm QCD}\approx 5.5$ and $m_g^{\rm KS}/\Lambda_{\rm QCD}\approx 7.7$. Second, provided the consistency relation is correct, either the value $\Lambda_{\rm QCD}=100$ MeV is inconsistently low when gluon-mass effects are included (Cornwall considers $\Lambda_{\rm QCD}=300$ MeV to be the appropriate value for $m_g\approx 500$ MeV) or the effective gluon mass is overestimated in all three models. Finally, one should take care that the introduction of an additional IR cutoff is compatible with the choice of the normalization point μ_0 in the OPE (Ref. 54), for this is the scale where the effective coupling constant is normalized to unity, signalizing the breakdown of perturbative QCD (Ref. 55). Choosing $\Lambda_{\rm QCD}=180$ MeV, the normalization point is $\mu_0=0.36$ GeV, whereas SVZ (Ref. 18) prefer to use $\Lambda_{\rm QCD}=100$ MeV corresponding to $\mu_0=0.2$ GeV. These values have to be contrasted with the scales following from Ref. 30 where the IR cutoff sets on at $Q^2\approx 4m_g^2$ yielding to the normalization scales: 1.1 GeV (CZ, GS models) and 1.5 GeV (KS model).

The preceding discussion shows that the Cornwall parametrization of the effective coupling constant should be treated very carefully. Its straightforward application, without matching the intrinsic scales of the formalism, provides merely regularized form factors whose scaling behavior is improved because the Q^2 domain, where perturbative QCD is applicable, is artificially extended toward lower values.

IV. STABILITY ANALYSIS OF THE MOMENT SUM RULES

We pass on now to the more demanding problem of performing a stability analysis of the moment sum rules. The equation to be treated with respect to its stability is (2.20). The spectral density is parametrized in standard form using the narrow-resonance approximation:[5,33]

$$\frac{1}{\pi}\mathrm{Im}I^{(n_1n_2n_3)}(s)=r^{(n_1n_2n_3)}\delta(s-M_N^2)+\theta(s-s^{(n_1n_2n_3)})\frac{\beta_1^{(n_1n_2n_3)}}{640\pi^4}s \ . \quad (4.1)$$

The quantity $r^{(n_1n_2n_3)}$ is called the "residue"[5,33] and it is a measure for the transition amplitude of the proton (neutron) into the quark current in question. For every moment of Φ_N, the residue is given by[5]

$$r^{(n_1n_2n_3)}=|f_N|^2\Phi^{(n_1n_2n_3)}(\tfrac{1}{2}\Phi_N^{(100)}+T^{(100)}) \ . \quad (4.2)$$

In (4.1) the proton contribution to the imaginary part of the correlator is shown explicitly, while the θ function stands for the continuum. Considering the nucleon distribution amplitude Φ_N as known, the stability analysis of the sum rule for each moment $\Phi_N^{(n_1n_2n_3)}$ can be treated along the lines developed by Ioffe and Belyaev[33] for the determination of baryon and baryon-resonance masses (see also Ref. 56).

The intersection of the curves corresponding to the left- and the right-hand sides of Eq. (2.20) for a given moment determines a balance point of the sum rule with respect to the Borel parameter M (M^2 resembles the momentum scale Q^2). In order to ensure stability of the sum rule (i.e., to make its validity *locally insensitive* to the choice of M), not a single point of reconciliation is desired, but a whole stability region where the two sides of the sum rule (almost) coincide. This is not trivial, owing to the fact that the phenomenological part of the sum rule is saturated by the first resonances while its theoretical part takes into account a truncated Wilson expansion (in our case the twist-three contributions).

It is clear that optimization of the stability properties amounts to a balance of the sum rule in the greatest possible (continuous) interval of the Borel parameter. Then, the truncated contributions on both of its sides are dominated by the lowest-order terms and the sum rule itself becomes stationary under small variations of M. In general, not the whole M region determined this way is physically meaningful. The balance of the sum rule should be considered in a restricted M interval where, on the one hand the nonperturbative corrections do not exceed some desired level of magnitude, and on the other hand the contribution of the model continuum is moderate. The first condition restricts the permissible M values from below; the second one limits the M interval from above. Adopting the terminology of Ioffe and Belyaev, this interval will be designated by the symbol Ω. (Note however that we refer to the parameter M instead of M^2.)

The restrictions imposed in our stability analysis are (i) the nonperturbative corrections are allowed to contribute to the sum rule together no more than 40% of the perturbative term and (ii) the contribution of the continuum to the sum rule is less than 40% of the perturbative term.

Let us now be more specific. Two possibilities for the spectral density are considered. (i) The phenomenological part of the sum rule is saturated by the lowest resonance in the channel with the given quantum numbers, i.e., the nucleon (one-resonance model). Higher states are taken into account *implicitly* in a model continuum [second term on the right-hand side (RHS) of (4.1)] starting at $s^{(n_1n_2n_3)}$. The sum rule for each moment is then reconciled according to the conditions just described, regarding the nucleon residue as known. The optimal values of the nucleon mass M_N and the duality interval

TABLE VII. Results of the stability analysis of the sum rules for the moments of the nucleon distribution amplitude Φ_N^{GS}. The entries in the one-resonance model are the nucleon residues $r_N^{(n_1n_2n_3)}$. The entries in the two-resonance model are the nucleon residues and the nucleon mass M_N obtained in the one-resonance model. Note that always the largest residue of the "effective resonance" is used and the interval Ω refers to the two-resonance model.

		1-resonance model			2-resonance model			
$(n_1n_2n_3)$	$\Phi_{N/GS}^{(n_1n_2n_3)}$	$r_N^{(n_1n_2n_3)}$ (10^{-6} GeV^4)	$s^{(n_1n_2n_3)}$ (GeV^2)	M_N (GeV)	$s^{(n_1n_2n_3)}$ (GeV^2)	$r_R^{(n_1n_2n_3)}$ (10^{-6} GeV^4)	Ω Interval (GeV)	Stability
100	0.63	12.708	3.95	1.10	4.00	4.55–4.75	1.21–1.40	Stable
010	0.14	2.824	2.30	1.04	2.30	1.62–1.98	0.84–1.04	Stable
001	0.236	4.761	3.52	1.06	3.55	3.88–4.07	0.90–1.14	Stable
200	0.29	5.850	3.80	0.90	3.87	2.50–2.57	1.33–1.38	Reduced stability
020	0.032	0.645	1.70	0.81	1.72	1.12–1.29	0.75–0.92	Stable, nucleon mass too small
002	0.008	0.161						Unreliable
110	0.11	2.219	3.85	1.09	3.88	1.04–1.22	0.94–1.21	Stable
101	0.23	4.640	5.65	1.36	5.67	0.13–0.18	1.03–1.33	Stable duality interval and nucleon mass too large
011	−0.003	−0.061	2.25	1.02				Unreliable gluon-condensate correction too large

TABLE VIII. Results of the stability analysis of the sum rules for the moments of the nucleon distribution amplitude Φ_N^{CZ}. The entries are as in the case of the amplitude Φ_N^{GS} (Table VII). The numbers in parentheses are the values given by CZ (Ref. 5).

		1-resonance model			2-resonance model			
$(n_1n_2n_3)$	$\Phi_{N/CZ}^{(n_1n_2n_3)}$	$r_N^{(n_1n_2n_3)}$ (10^{-6} GeV^4)	$s^{(n_1n_2n_3)}$ (GeV^2)	M_N (GeV)	$s^{(n_1n_2n_3)}$ (GeV^2)	$r_R^{(n_1n_2n_3)}$ (10^{-6} GeV^4)	Ω Interval (GeV)	Stability
100	0.63	12.606	3.90	1.10	3.95	4.84–5.04	1.21–1.39	Stable
010	0.15	3.001	2.34	1.06	2.35	3.52–3.79	0.84–1.07	Stable
001	0.22	4.402	3.20	1.04	3.21	0.90–1.48	0.90–1.14	Stable
200	0.40	8.004	3.95	1.16	4.08	2.37–2.44	1.33–1.42	Reduced stability, nucleon mass unreliable
020	0.024 (0.025)	0.480	1.34	0.78	1.35	0.38–0.44	0.75–0.82	Unreliable, continuum contribution dominates
002	0.08	1.601	3.26	0.91	3.27	0.12–0.49	0.99–1.27	Reduced stability
110	0.11	2.201	3.76	1.09	3.79	1.06–1.21	0.94–1.21	Stable
101	0.123	2.461	3.64	1.10	3.67	0.77–0.83	1.03–1.34	Stable
011	0.017 (0.027)	0.340	2.85	0.91	2.90	1.94–2.27	1.13–1.19	Unstable

$s^{(n_1n_2n_3)}$ are those which minimize the disparity between the two sides of the sum rule in the largest stability interval. (ii) In addition to the nucleon, an "effective resonance" with mass $M_R=1.5$ GeV and residue $r_R^{(n_1n_2n_3)}$ is taken into account *explicitly* in the spectral density (two-resonance model). In this case, the left-hand side (LHS) of (2.20) reads

$$4[r_N^{(n_1n_2n_3)}\exp(-M_N^2/N^2)+r_R^{(n_1n_2n_3)}\exp(-M_R^2/N^2)] \tag{4.3}$$

and the RHS of (4.1) receives an additional contribution equal to $r_R^{(n_1n_2n_3)}\delta(s-M_R^2)$. The corresponding sum rules are fitted in the same M interval as before using as inputs the nucleon mass and the nucleon residue found in (i). Optimal stability is now achieved for continuum thresholds $s_R^{(n_1n_2n_3)}$ equal to or slightly larger than those of the one-resonance model. In addition, the range of residues $r_R^{(n_1n_2n_3)}$ of the "effective resonance" for each sum rule is also determined. Note that for both cases $|f_N|=5.2\times10^{-3}$ GeV^2 and the condensates have the values given in (1.2).

The results for both saturation cases are compiled in Table VII (GS model) and Table VIII (CZ model). The graphical representations versus M of Eq. (2.20) evaluated for the moments of the model distribution amplitudes are shown in Figs. 8–10.

In discussing these results we first remark that they are correct modulo logarithmic corrections due to the anomalous dimensions of the involved operators. This is because in general each sum rule is reconciled at a different momentum scale. Ignoring this shift in scales in favor of an average normalization point, our analysis yields $\bar{\mu}\approx1.1$ GeV for both nucleon distribution amplitudes. From examining Fig. 8 in conjunction with Tables VII and VIII it is obvious that, at the level of the linear moments, both considered models have stability properties which resemble one another. It is worth noting that the stability intervals exceed the region Ω where our imposed

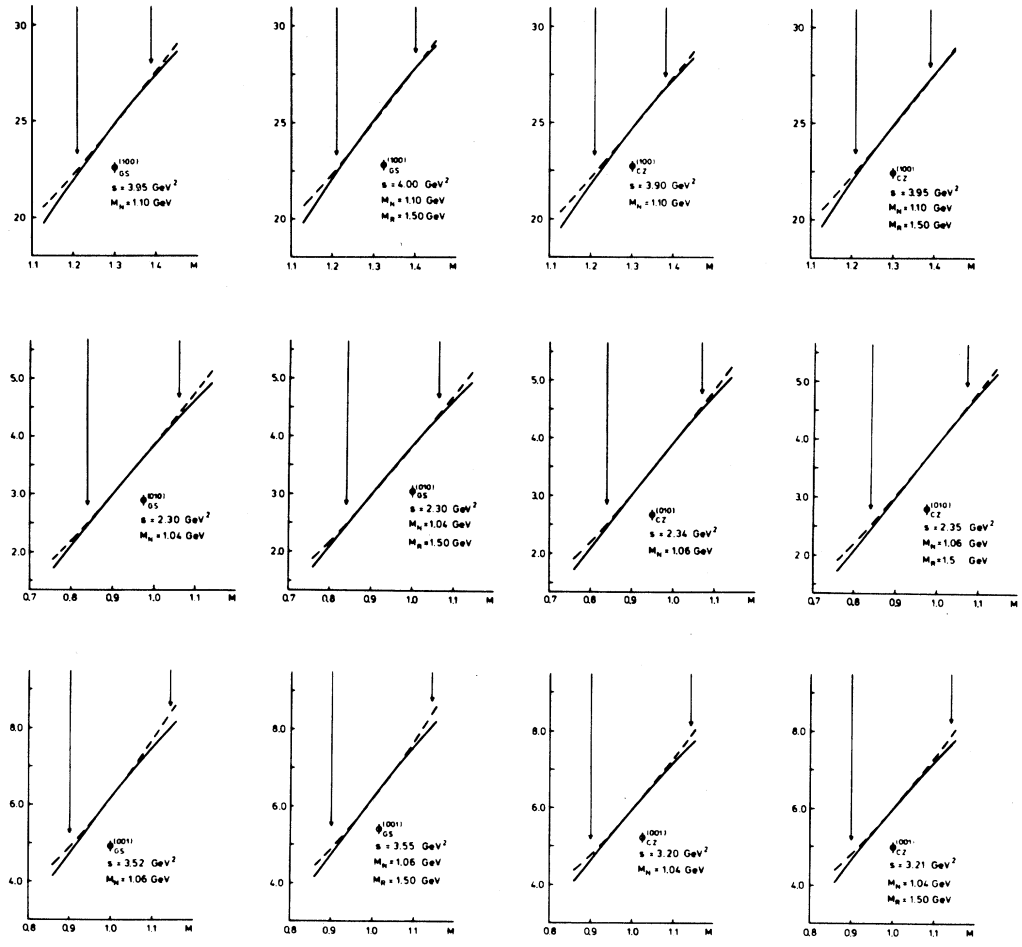

FIG. 8. Plots versus M of the sum rules for the linear moments of the nucleon distribution amplitudes Φ_N^{GS} and Φ_N^{CZ} saturating the phenomenological side (denoted by a solid line) by one resonance (nucleon) and two resonances (nucleon + "effective resonance" with $M_R=1.5$ GeV). The theoretical side of the sum rules is represented by a dashed line, and the interval Ω is marked by arrows. The optimal values of the nucleon mass and the duality intervals are also shown.

conditions are satisfied.[58] The two models are differentiated by analyzing the stability properties of the sum rules for the bilinear moments. Here the stability criterion provides a useful tool to check the reliability of the model distribution amplitudes in terms of their moments. For example, we find that the agreement of the sum rule for the moment $\Phi_N^{(011)}$ is only marginal, although both models give moment values within the range estimated by CZ. Thus we conclude that this sum rule should not be taken very seriously in the determination of nucleon distribution amplitudes. It is also important to appreciate that the tiny value of the moment $\Phi_{N/GS}^{(002)}$, which is by an order of magnitude smaller than needed to match its sum rule, is in fact a *prediction* of the GS model, since it is an *unavoidable* consequence of minimizing the ratio $|F_1^n/F_1^p|$.

Summarizing the results of this section the following points are worth emphasizing. (i) Comparison shows that the mean values $\overline{s}^{(n_1 n_2 n_3)}$ given by CZ (Ref. 5) for the duality intervals are for most of the sum rules systematically smaller than the optimal values obtained in this work. (ii) Averaging over all values obtained for the nucleon mass in optimizing the stability of the sum rule for each moment, one finds very reasonable results: $\overline{M}_N^{\rm GS}=1.0^{+0.36}_{-0.19}$ GeV and $\overline{M}_N^{\rm CZ}=1.02^{+0.14}_{-0.24}$ GeV. (iii) The characteristic momentum scale where most of the sum rules can be reconciled is $\overline{M}\geq 1.1$ GeV for both considered models of nucleon distribution amplitudes. This scale represents an optimal choice for the renormalization point, since for such momenta the nucleon can still be viewed as an "elementary" particle. For smaller M values, nonperturbative operators occurring with inverse powers of M^2 con-

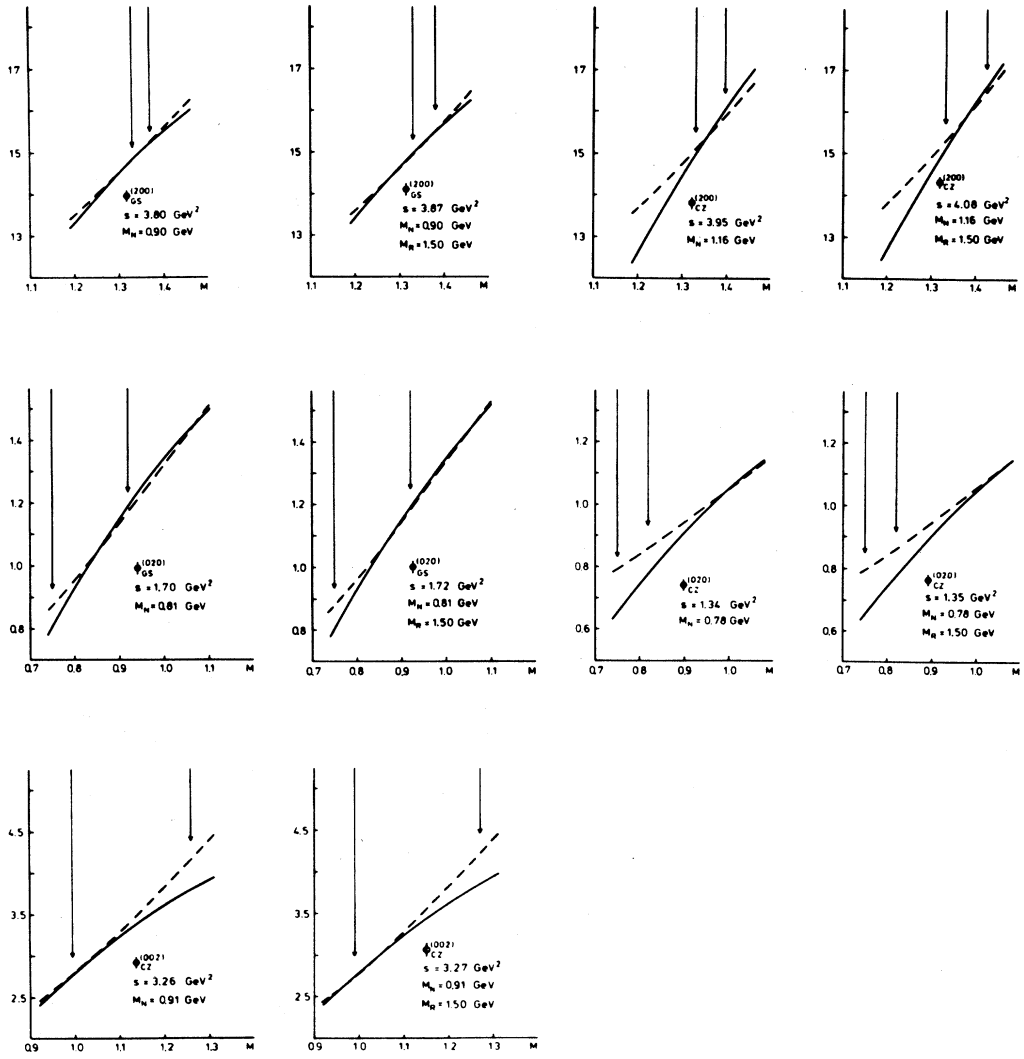

FIG. 9. Plots versus M of the sum rules for the bilinear moments (one $n_i=2$) of the amplitudes $\Phi_N^{\rm GS}$ and $\Phi_N^{\rm CZ}$. The designations are the same as in Fig. 8.

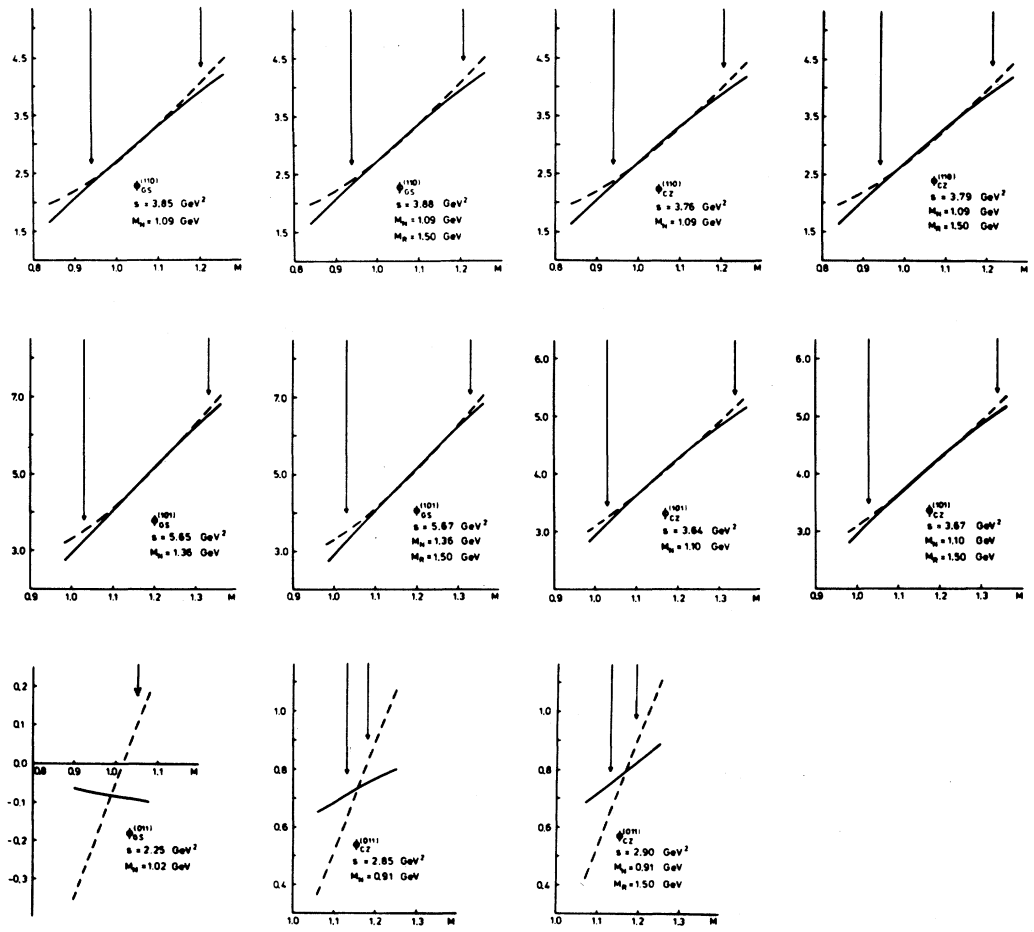

FIG. 10. Plots versus M of the sum rules for the bilinear moments $(n_i,n_j=0,1)$ of the amplitudes $\Phi_N^{\rm GS}$ and $\Phi_N^{\rm CZ}$. The designations are the same as in Fig. 8.

tribute increasingly large corrections, while for $M^2 \gg 1.21$ GeV^2 contamination due to higher resonances cannot be disregarded. For twist three, the dominant contributions to the sum rules[5] at low momenta are due to the four-quark condensate. Bearing this fact in mind, one should be very cautious when attempting to combine the sum-rule results[5,15,16] with Cornwall's framework where the nonperturbative structure of the QCD vacuum is mainly attributed to the gluon condensate (gluon-vortex formation[50]).

V. ON THE PROBABILISTIC INTERPRETATION OF THE NUCLEON DISTRIBUTION AMPLITUDE ϕ_N

As discussed in Sec. III, the nucleon distribution amplitude $\Phi_N(x_i,\mu^2) \sim \int^{\mu^2}[d^2k_\perp]\psi(x_i,\mathbf{k}_{\perp i})$, which specifies the longitudinal-momentum distributions of the valence quarks collinear up to the scale μ^2, has for both considered models a complex structure with positive and negative domains (Fig. 2). Thus, despite the fact that $\Phi_N(x_i,\mu^2)$ is normalized to unity [Eq. (3.17)], *it is not a (probability) density* because it is not a non-negative distribution. For this reason, the bona fide probabilistic interpretation of the moments of this amplitude, although popular[5,16,30] and perhaps tentative, it is, in fact, mathematically incorrect.

Intending to interpret the information contained in $\Phi_N(x_i,\mu^2)$ in a probabilistic way, we recall that the quark probability distribution is given by[1]

$$q(x_i,\mu^2) \sim \int^{k_{\perp i}^2 \le \mu^2} [d^2k_\perp]|\psi(x_i,\mathbf{k}_{\perp i})|^2 \tag{5.1}$$

with the normalization condition

$$\int_0^1 [dx] q(x_i,\mu^2) = P_{3q} \ , \tag{5.2}$$

where P_{3q} is the probability for finding three valence quarks in the nucleon. Unfortunately, the Fock-state wave functions $\psi(x_i,\mathbf{k}_{\perp i})$, which potentially describe all hadronic matrix elements, cannot be computed from first principles. Thus, one has to resort either to some phenomenological ansatz for $\psi(x_i,\mathbf{k}_{\perp i})$ or having recourse to $\Phi_N(x_i,\mu^2)$ make some plausible assumptions concerning Eq. (5.1).

In this paper we follow the second option and consider expectation values of the longitudinal-momentum fractions with respect to the density[59] $|\Phi_N(x_i,\mu^2)|^2$:

$$\langle x_1^{n_1} x_2^{n_2} x_3^{n_3} \rangle = N^{-1} \int_0^1 [dx] |\Phi_N(x_i,\mu^2)|^2 x_1^{n_1} x_2^{n_2} x_3^{n_3} \tag{5.3}$$

with normalization

$$N \equiv \int_0^1 [dx] |\Phi_N(x_i,\mu^2)|^2 \, . \tag{5.4}$$

Of course, the density $|\Phi_N(x_i,\mu^2)|^2$ is not directly related to the quark probability distribution $q(x_i,\mu^2)$, since the last one contains the square of the Fock-state wave function $\psi(x_i,\mathbf{k}_{1i})$ before, not after, integrating over the transverse momenta. Nevertheless, $|\Phi_N(x_i,\mu^2)|^2$ is a mathematically reasonable density and thus expectation values according to (5.3) provide a measure for the partition of the longitudinal momentum of the proton (neutron) among the valence quarks. In addition, these expectation values have the physical virtue of depending on the *same* reference momentum as the corresponding moments [Eq. (3.6)]. Since no additional assumptions are made, this recipe ensures that the physical content of the moments *effectively* translates into that of the expectation values.

The results for the (normalized) expectation values of the longitudinal-momentum fractions x_i with respect to $\Phi_N^{\rm GS}$ and $\Phi_N^{\rm CZ}$ are given in Table IX. By comparing these results with those obtained for the moments (Tables VII and VIII), one realizes that the strong asymmetry indicated by the moments is considerably reduced. In fact, the main effect of taking expectation values $\langle x_1^{n_1} x_2^{n_2} x_3^{n_3} \rangle$ instead of moments $\Phi_N^{(n_1 n_2 n_3)}$ is a *leveling* of the longitudinal-momentum fractions carried by the quarks.

Concerning the CZ distribution amplitude, the physical picture emerging from expectation values is, in principle, the same as that already suggested[5] on the basis of the corresponding moments. We find $\langle x_1 \rangle \approx 3\langle x_{2(3)} \rangle$, and $\langle x_1^2 \rangle \approx 7\langle x_{2(3)}^2 \rangle$, while the differences between the joint expectation values $\langle x_1 x_2 \rangle$, $\langle x_1 x_3 \rangle$, $\langle x_2 x_3 \rangle$, and the corresponding moments are negligible (compare Tables VIII and IX). We may summarize all that by the statement that the CZ distribution amplitude is indeed dominated by one up quark having the same helicity as the proton and carrying nearly 60% of its longitudinal momentum; the remaining two quarks sharing almost equal fractions of longitudinal momentum.

TABLE IX. Normalized expectation values of the longitudinal-momentum-fractions x_i with respect to the densities $|\Phi_N^{\rm GS}|^2$ and $|\Phi_N^{\rm CZ}|^2$.

$n_1 n_2 n_3$	$\langle x_1^{n_1} x_2^{n_2} x_3^{n_3} \rangle_{\rm GS}$	$\langle x_1^{n_1} x_2^{n_2} x_3^{n_3} \rangle_{\rm CZ}$
000	1.0	1.0
100	0.373	0.591
010	0.211	0.201
001	0.416	0.209
200	0.167	0.370
020	0.059	0.052
002	0.193	0.058
110	0.068	0.110
101	0.138	0.112
011	0.084	0.040

The crucial distinction between moments and expectation values shows up in the case of the GS distribution amplitude. As seen in Sec. IV, the values of the linear moments of $\Phi_N^{\rm GS}$ almost coincide with those of $\Phi_N^{\rm CZ}$. Trusting to the probabilistic interpretation of moments, one would tend to draw the same conclusions for the GS amplitude as for the CZ one. On the other hand, we have shown in Sec. III that these amplitudes have fundamentally different structures. Taking expectation values instead of moments, we find $\langle x_1 \rangle \approx \langle x_3 \rangle \approx 2\langle x_2 \rangle$, i.e., an equipartition of longitudinal momentum between the first up quark and the down quark within the proton. Remarkably, the expectation value $\langle x_3^2 \rangle$ which corresponds to the extremely small value $\Phi_{N/\rm GS}^{(002)} = 0.008$ turns out to be of the same order of magnitude as $\langle x_1^2 \rangle$, while $\langle x_2^2 \rangle$ is nearly three times smaller. As estimates for the joint expectation values, we obtain $\langle x_1 x_3 \rangle \approx 2\langle x_1 x_2 \rangle \approx 2\langle x_2 x_3 \rangle$ in agreement with $\Phi_{N/\rm GS}^{(101)} \approx 2\Phi_{N/\rm GS}^{(110)}$ and in contrast to $\Phi_{N/\rm GS}^{(101)} \gg |\Phi_{N/\rm GS}^{(011)}|$ (compare Tables VII and IX). Thus, under our simplifying assumptions, the quark combination $u^{\uparrow}(x_1) d^{\uparrow}(x_3)$ [or $u^{\uparrow}(x_1) u^{\uparrow}(x_2)$; remember Eq. (2.10)] seems to carry most of the proton's longitudinal momentum. On the other hand, the joint expectation values obtained in the case of the CZ model are $\langle x_1 x_2 \rangle \approx \langle x_1 x_3 \rangle \approx 3\langle x_2 x_3 \rangle$ suggesting that the quark combinations $u^{\uparrow}(x_1) u^{\downarrow}(x_2)$ and $u^{\uparrow}(x_1) d^{\uparrow}(x_3)$ share almost equal fractions of longitudinal momentum. [This partition of x favors dominance of $u^{\uparrow}(x_1)$ in the proton, as said above.]

Combining these results, we claim that the GS distribution amplitude may be viewed as indicating the existence of a diquark cluster within the proton having spin one with helicity parallel to the proton's helicity and carrying almost 80% of its longitudinal momentum.

VI. SUMMARY AND CONCLUSIONS

In this paper we have elaborated on the quark content of the nucleon using perturbative light-cone QCD[1,2] supplemented by QCD sum rules.[18,5] Based on the formalism described in Sec. II, we have outlined in Sec. III the arguments underlying the model distribution amplitude $\Phi_N^{\rm GS}$ proposed in Refs. 15 and 22. The determination of the expansion coefficients B_n in the Appell polynomial decomposition of the nucleon distribution amplitude has been treated in detail. We have found that relying in ansatz (3.4) solely on the first three Appell polynomials $\tilde{\Phi}_0, \tilde{\Phi}_1, \tilde{\Phi}_2$, the nucleon distribution amplitude is forced by the moment sum rules[5] to have the structure of $\Phi_N^{\rm CZ}$. Conversely, relative dominance of the second-order Appell polynomials $\tilde{\Phi}_3, \tilde{\Phi}_4, \tilde{\Phi}_5$ in (3.4) leads rather to the structure of $\Phi_N^{\rm GS}$.

Both proposed[5,15] model distribution amplitudes, shown in Fig. 2, though, in fact, rudimentary, do incorporate genuine nonperturbative contributions, which are indispensable for a realistic description of the nucleon. Indeed, using these amplitudes we have calculated the proton Dirac form factor in reasonable agreement with the data (see Fig. 6) although this agreement depends in a crucial way on the treatment of the effective coupling constant $\alpha_s(Q^2)$ and the choice of the scale parameter

$\Lambda_{\rm QCD}$. In the case of the neutron, however, the form-factor predictions made by the two models are diametrically different. While the CZ model predicts sizable values for F_1^n in the intermediate Q^2 region, the GS model requires an almost vanishing F_1^n in the whole Q^2 range (see Table VI and Fig. 7). High-precision data at intermediate Q^2 values will surely help to differentiate the two models.[32] Closing Sec. III we have shown that attempts[30] to combine sum-rule results with Cornwall's parametrization of the effective coupling constant should be treated very carefully.

Trying to understand the quality of the model distribution amplitudes $\Phi_N^{\rm CZ}$ and $\Phi_N^{\rm GS}$ from a more theoretical viewpoint, we have performed in Sec. VI a stability analysis of the moment sum rules, relying on the Wilson coefficients calculated by CZ (Ref. 5). This analysis provides the possibility to estimate the range of the residues of the "effective resonance" (Tables VII and VIII) and can serve as a guide in modeling distribution amplitudes, since it reveals the trends along which optimized values of the expansion coefficients B_n can be obtained.

Finally, in Sec. V we have raised objections against the popular[5,16,30] probabilistic interpretation of moments and have suggested instead to consider expectation values of the longitudinal-momentum fractions x_i with respect to the density $|\Phi_N(x_i,\mu^2)|^2$ (Table IX). According to the physical picture emerging from this (simplifying) treatment, the CZ distribution amplitude is dominated by an up quark with the same helicity as the proton. On the other hand, the GS distribution amplitude is rather compatible with the idea of a diquark cluster within the proton. Testable consequences of this picture will be considered elsewhere.

Note added. After completion of the present investigation I received a paper by Carlson and Poor[60] which deals with expectation values of longitudinal-momentum fractions relying on the assumption that in $\psi(x_i,\mathbf{k}_{\perp i})$ the transverse-momentum dependence and the dependence on the longitudinal-momentum fractions factorize. This is an interesting attempt, but it is not obvious how the intrinsic dependence of the amplitude $\Phi_N(x_i,\mu^2)$ on the normalization scale μ^2 can be accounted for in their framework.

ACKNOWLEDGMENTS

I would like to thank Joachim Holz and Wulf Krümpelmann for useful suggestions concerning the computer calculations.

[1]G. P. Lepage and S. J. Brodsky, Phys. Lett. **87B**, 359 (1979); Phys. Rev. Lett. **43**, 545 (1979); **43**, 1625(E) (1979); Phys. Rev. D **22**, 2157 (1980).

[2]V. A. Avdeenko, S. E. Korenblit, and V. L. Chernyak, Yad. Fiz. **33**, 481 (1981) [Sov. J. Nucl. Phys. **33**, 252 (1981)].

[3]P. H. Damgaard, Nucl. Phys. **B211**, 435 (1983); G. R. Farrar, E. Maina, and F. Neri, *ibid.* **B259**, 702 (1985); **B263**, 746(E) (1986); J. Gunion and D. Millers, Phys. Rev. D **34**, 2657 (1986).

[4]P. H. Damgaard, K. Tsokos, and E. Berger, Nucl. Phys. **B259**, 285 (1985), and references therein.

[5]V. L. Chernyak and I. R. Zhitnitsky, Nucl. Phys. **B246**, 52 (1984); V. L. Chernyak and A. R. Zhitnitsky, Phys. Rep. **112**, 173 (1984).

[6]C. E. Carlson and J. L. Poor, Phys. Rev. D **34**, 1478 (1985); **36**, 2169 (1987).

[7]C. E. Carlson, Phys. Rev. D **34**, 2704 (1986).

[8]S. J. Brodsky and G. R. Farrar, Phys. Rev. Lett. **31**, 1153 (1973); Phys. Rev. D **11**, 1309 (1975).

[9]S. J. Brodsky *et al.*, Phys. Lett. **91B**, 239 (1980).

[10]A. Duncan and A. H. Mueller, Phys. Lett. **90B**, 159 (1980); Phys. Rev. D **21**, 1636 (1980); A. Efremov and A. Radyushkin, Teor. Mat. Fiz. **42**, 167 (1980); Phys. Lett. **94B**, 245 (1980).

[11]A complete proof of factorization for elastic scattering in perturbative QCD is still lacking.

[12]K. G. Wilson, Phys. Rev. **179**, 1499 (1969).

[13]In order to avoid unphysical degrees of freedom in the Fock-state components, the light-cone gauge $A^+ = A^0 + A^3 = 0$ is used.

[14]N. Isgur and C. H. Llewellyn Smith, Phys. Rev. Lett. **52**, 1080 (1984); O. J. Jacob and L. S. Kisslinger, *ibid.* **56**, 225 (1986).

[15]M. Gari and N. G. Stefanis, Phys. Lett. B **175**, 462 (1986).

[16]I. D. King and C. T. Sachrajda, Nucl. Phys. **B279**, 785 (1987).

[17]Improvements in the numerical evaluation of moments of distribution amplitudes using lattice gauge theory are promising, but technically complex and still incomplete. Results for the pion are given in A. S. Kronfeld and D. M. Photiadis, Phys. Rev. D **31**, 2939 (1985); S. Gottlieb and A. S. Kronfeld, Phys. Rev. Lett. **55**, 2531 (1985); Phys. Rev. D **33**, 227 (1986). In the case of the proton, the first three moments of $\Phi_N(x_i,Q^2)$, and the "proton decay constant" f_N, important for grand unified theories, have been recently computed in D. G. Richards, C. T. Sachrajda, and C. J. Scott, Nucl. Phys. **B286**, 683 (1987).

[18]M. A. Shifman, A. I. Vainshtein, and V. I. Zakharov, Phys. Rev. Lett. **42**, 297 (1979); Nucl. Phys. **B147**, 385 (1979); **B147**, 448 (1979); **B147**, 519 (1979).

[19]It is assumed that perturbative contributions to vacuum condensates are absent.

[20]V. L. Chernyak and V. R. Zhitnitsky, Nucl. Phys. **B201**, 492 (1982); V. L. Chernyak, A. R. Zhitnitsky, and I. R. Zhitnitsky, *ibid.* **B204**, 477 (1982).

[21]See, e.g., J. A. Shohat and J. D. Tamarkin, *The Problem of Moments* (Am. Math. Soc., New York, 1943); N. I. Akhiezer, *The Classical Moment Problem* (Oliver and Boyd, London, 1965).

[22]M. Gari and N. G. Stefanis, Phys. Rev. D **35**, 1074 (1987).

[23]N. S. Craigie and J. Stern, Nucl. Phys. **B216**, 209 (1983).

[24]M. J. Lavelle, Nucl. Phys. **B260**, 323 (1985).

[25]Higher-order moments of distribution amplitudes correspond to operator products containing higher derivatives which in turn probe larger distances.

[26]K. Tesima, Phys. Lett. **110B**, 319 (1982).

[27]R. G. Arnold *et al.*, Phys. Rev. Lett. **57**, 174 (1986).
[28]M. Gari and W. Krümpelmann, Z. Phys. A **322**, 689 (1985).
[29]J. G. Körner and M. Kuroda, Phys. Rev. D **16**, 2165 (1977); R. G. Arnold, C. E. Carlson, and F. Gross, Phys. Rev. C **21**, 1426 (1980).
[30]C.-R. Ji, A. F. Sill, and R. M. Lombard-Nelsen, Phys. Rev. D **36**, 165 (1987).
[31]C. E. Carlson, M. Gari, and N. G. Stefanis, Phys. Rev. Lett. **58**, 1308 (1987).
[32]M. Gari and W. Krümpelmann, Phys. Lett. B **173**, 10 (1986); R. G. Arnold (private communication).
[33]B. L. Ioffe, Nucl. Phys. **B188**, 317 (1981); **B191**, 591(E) (1981); V. M. Belyaev and B. L. Ioffe, Zh. Eksp. Teor. Fiz. **83**, 876 (1982) [Sov. Phys. JETP **56**, 493 (1982)].
[34]A. Erdelyi *et al.*, *Higher Transcendental Functions* (McGraw-Hill, New York, 1953), Vol. II.
[35]M. E. Peskin, Phys. Lett. **88B**, 128 (1979).
[36]M. Kremer, Nucl. Phys. **B168**, 272 (1980).
[37]Normal ordering of the quantum field operators in (2.6) is implemented.
[38]The covariant analog of the light-cone gauge is the gauge $a=-3$ discussed in N. S. Craigie and H. Dorn, Nucl. Phys. **B185**, 204 (1981); N. G. Stefanis, Nuovo Cimento **83A**, 205 (1984).
[39]A. B. Henriques, B. H. Kellet, and R. G. Moorhouse, Ann. Phys. (N.Y.) **93**, 125 (1975). Notice however that we use the notation of Ref. 5.
[40]For brevity the same symbols are used here and below to denote operators and their matrix elements. This should not cause confusion.
[41]The choice of baryonic currents is somewhat ambiguous. Optimal choices have been proposed, selected to give minimal coupling to the continuum. See, e.g., Ref. 33, and Y. Chung *et al.*, Nucl. Phys. **B197**, 55 (1982); Z. Phys. C **15**, 367 (1982).
[42]Since the nucleon distribution amplitude is a gauge-invariant quantity, any appropriate gauge can be used in the calculations.
[43]Note that the discussion of ansatz (3.4) in Refs. 15 and 22 is misleading.
[44]The relation $\sum_{i=1}^{3} x_i = 1$ has been used to obtain the presented form from the original one (see Ref. 1). Note also that the polynomial $\tilde{\Phi}_2$ used here has an opposite overall sign compared to the polynomial $\tilde{\Phi}_2$ given in Ref. 1. This has no physical significance, since the sign can be absorbed in the expansion coefficient B_2.
[45]To facilitate comparison with other works, note that the expansion coefficients B_n used here and those defined by Brodsky and Lepage in Ref. 1 are related by $120(B_i/N_i)=a_i$
[46]M. F. Gari and N. G. Stefanis, Phys. Lett. B **187**, 401 (1987).
[47]R. G. Arnold *et al.*, Phys. Rev. Lett. **57**, 174 (1986); P. N. Kirk *et al.*, Phys. Rev. D **8**, 63 (1973); W. Albrecht *et al.*, Phys. Lett. **26B**, 642 (1968); S. Rock *et al.*, Phys. Rev. Lett. **49**, 1139 (1982); G. G. Simon *et al.*, Z. Naturforsch. **35a**, 1 (1980); G. Höhler *et al.*, Nucl. Phys. **B114**, 505 (1976); M. D. Mestayer, Ph.D. thesis, Stanford University, Report No. SLAC-214, 1978; W. B. Atwood, Ph.D. thesis, Stanford University, Report No. SLAC-185, 1975.
[48]Strictly speaking, the scale parameter $\Lambda_{\rm QCD}$ can be defined precisely only when at least the two-loop corrections are taken into account. The reason is that for $\alpha_s \to 0$ the one-loop expression for $\Lambda_{\rm QCD}$ obtained by inverting Eq. (3.20) develops an essential singularity [M. Bace, Phys. Lett. **78B**, 132 (1978)].
[49]The reference momentum $Q^2=20$ GeV^2 is chosen so that $\ln(Q^2/\Lambda^2_{\rm QCD})$ is near the middle of the range covered by the high-Q^2 data, but the solutions are only slightly modified if other values $Q^2 \gg \mu^2$ are used.
[50]J. M. Cornwall, Phys. Rev. D **26**, 1453 (1982). See also G. Parisi and R. Petronzio, Phys. Lett. **94B**, 51 (1980).
[51]R. Petronzio, Lectures at the 1984 CERN School of Physics, Lofthus, Hardanger, Norway, 1984 (unpublished).
[52]Actually, $m_g^2=0.3$ GeV^2 yields the optimal fit for the CZ model, whereas the form factors of the GS model are somewhat overestimated.
[53]J. M. Cornwall and A. Soni, Phys. Lett. **120B**, 431 (1982).
[54]Especially the factorization hypothesis underlying the reduction of higher-dimensional condensates requires a low normalization point, $\mu_0 \sim R_{\rm conf}^{-1}$, where $\alpha_s(\mu_0) \sim 1$ (second paper in Ref. 18). In practice, a larger normalization point ($\mu_0=0.5$ GeV) is used, corresponding to a smaller value of α_s (see, e.g., Ref. 33).
[55]Choosing μ_0 to be large ensures theoretical control over the perturbative contributions because $\alpha_s(\mu_0) \ll 1$. On the other hand, one would like to choose μ_0 as low as posssible, in order to prevent contamination of the nonperturbative corrections by perturbative contributions. The optimal choice lies in the "window" where both requirements on μ_0 are satisfied simultaneously. That such a "window" does exist for QCD was shown by the ITEP group in Ref. 18; see also V. A. Novikov *et al.*, Nucl. Phys. **B249**, 445 (1985).
[56]Y. Chung *et al.*, Z. Phys. C **25**, 151 (1984).
[57]From the sum rules for $V_{\rm GS}^{(000)}$, $V_{\rm GS}^{(001)}$, $\Phi_{N/{\rm GS}}^{(100)}$, and Eq. (2.10), one easily verifies that the "proton decay constant" is $|f_N|=5.2\times10^{-3}$ GeV^2 (the values $M_N=1.0$ GeV, $M=1.18$ GeV, and $s=3.95$ GeV^2 are used).
[58]The good agreement at higher M values confirms the assumption that the higher states can be approximated well enough by the continuum.
[59]Expectation values with respect to the distribution amplitude $T(x_i,\mu^2)$ can be easily computed using the relation

$$2\langle x_1^{n_1} x_2^{n_2} x_3^{n_3} \rangle_T = \langle x_1^{n_1} x_2^{n_3} x_3^{n_2} \rangle_{\Phi_N} + \langle x_1^{n_2} x_2^{n_3} x_3^{n_1} \rangle_{\Phi_N} ,$$

which follows from Eq. (2.10).
[60]C. E. Carlson and J. L. Poor, Phys. Rev. D **36**, 2070 (1987).